PHYSICAL REVIEW D VOLUME 16, NUMBER 3 1 AUGUST 1977

Unitary coupled-channel analysis of diffractive production of the A_1 resonance

J. L. Basdevant
Laboratoire de Physique Théorique et Hautes Energies, Université Pierre et Marie Curie, Paris, France*

Edmond L. Berger
CERN, Geneva, Switzerland
and High Energy Physics Division,† Argonne National Laboratory, Argonne, Illinois 60439
(Received 11 April 1977)

Employing unitary coupled-channel $J^{PC} = 1^{++}$ partial-wave amplitudes for the $\rho\pi$ and $K^*\bar{K}$ systems, we show that the mass dependence and phase variations of the diffractive data on $\pi p \to (\rho\pi)p$ are indicative of the presence of an A_1 resonance whose mass and width we determine to be roughly 1.3 ± 0.15 GeV and 400 ± 100 MeV, respectively. Our unitary amplitudes incorporate the Deck backgrounds explicitly. The fits to the data are excellent. We point out some interesting quantities to be measured in the future in order to resolve remaining uncertainties.

I. INTRODUCTION

The A_1 resonance and its partners in the $J^{PC} = 1^{++}$ SU(3) nonet remain one of the enigmas of meson spectroscopy.[1] A broad enhancement centered near $M = 1.1$ GeV in the $\rho\pi$ mass spectrum is observed in the diffractive process $\pi p \to (\rho\pi)p$. The structure has the desirable quantum numbers $J^P = 1^+$, with the $\rho\pi$ system in an S wave, and has roughly the "expected" mass. However, as the mass of the $\rho\pi$ system is varied, the phase of the 1^+ wave changes slowly with respect to other partial waves,[2] unlike the rapid behavior expected of a Breit-Wigner A_1 amplitude. Complicating the interpretation is the fact that many features of the data can be explained qualitatively as a kinematical (or background) Deck enhancement.[3] In this article we present a new analysis of the A_1 resonance region observed in diffractive production. We begin with the assumption that a calculable and reasonably well defined Deck background is present in the $J^P = 1^+$ partial wave. We then calculate the unitarity "corrections" to this Deck amplitude by taking into account the behavior of the $\rho\pi \to \rho\pi$ scattering amplitude and its attendant rescattering corrections, using the techniques of final-state interactions.[4,5] Our amplitudes are properly analytic and obey unitarity; there is no "double-counting." A crucial new feature of our approach is that we consider both the $\rho\pi$ and $K^*\bar{K}$ coupled decay channels of the A_1. We show that inelasticity, in terms of the $K^*\bar{K}$ channel, may be directly responsible for the modest phase variation observed in the $J^P = 1^+$ $\rho\pi$ wave in the resonance region. We find that certain critical aspects of the diffractive data are explained naturally if we invoke an A_1 resonance in interference with the Deck background. These include absolute normalization, the structure of $d\sigma/dM$, and the phase of the 1^+ amplitude.

Our A_1 resonance is broad, with $M_{A_1} = 1.3 \pm 0.15$ GeV and $\Gamma_{A_1} = 0.4 \pm 0.1$ GeV. The assumption that the $\rho\pi$ amplitude does not resonate can be discarded with good confidence. However, we also stress certain critical aspects of the data which deserve to be improved in order to make more precise quantitative statements possible.

There are two principal components in our approach. First, we require the Deck production amplitudes for the $J^P = 1^+$ partial wave of the $\rho\pi$ system in $\pi p \to (\rho\pi)p$, and for the $J^P = 1^+$ $K^*\bar{K}$ system in $\pi p \to (K^*\bar{K})p$. Second, we develop a parametrization of the coupled-channel scattering amplitudes for $\rho\pi \to \rho\pi$, $\rho\pi \to K^*\bar{K}$, and $K^*\bar{K} \to K^*\bar{K}$. Given the Deck amplitudes and the $2 \leftrightarrow 2$ coupled-channel vector pseudoscalar scattering amplitudes, the rest of our problem is a proper implementation of the requisites of unitarity. Unitarity and analyticity permit us to establish the form for the unitary coupled-channel partial-wave Deck amplitudes for diffractive production of the A_1 region. The diffractive data can then be used to determine the parameters of the $\rho\pi \to \rho\pi$ and $K^*\bar{K} \to K^*\bar{K}$ scattering amplitudes, including, in particular, the possible presence of a resonance.

While developed for the A_1 channel, our method is easily generalized to other diffractive production processes including, for example, $\pi p \to A_3 p$, $pp \to N^*(1400)p$, and $Kp \to Qp$, where the relevant coupled channels may be $A_3 \to (f\pi, K^*(1420)\bar{K})$, $N^*(1400) \to (N\pi, \Delta\pi)$, and $Q \to (K^*\pi, \rho K,$ and $\omega K)$.

In Sec. II we describe our Deck amplitudes and discuss how theoretical predictions are compared with experimental spectra. In Sec. III we explain

fully our method for incorporating unitarity corrections, and we provide analytic forms for the resulting amplitudes. Section IV contains our numerical results, and finally, in Sec. V we discuss these results and present concluding remarks.

II. BACKGROUND DECK AMPLITUDES

A. Generalities

The Deck amplitudes which contribute to the diffractive production of the nonresonant $\rho\pi$ system are well known.[3,6] Diagrams are shown in Figs. 1(a) and 1(b). The pion-exchange amplitude of Fig. 1(a) contributes a term to the total invariant amplitude having the form

$$T_D^{\pi} = g_{\rho\pi\pi} K_\rho(t_2) \frac{1}{m_\pi^2 - t_2} i s_{13} e^{bt_1} \sigma_{\pi p}. \tag{2.1}$$

Here $g_{\rho\pi\pi}$ is the $\rho\pi\pi$ coupling constant, $K_\rho(t_2)$ is the incident pion momentum in the ρ rest frame, b is the slope of the πN elastic diffraction peak, and $\sigma_{\pi p}$ is the πp total cross section. The invariants s_{13}, t_1, and t_2 are defined in Fig. 1(a). For similicity in the above equation we have not introduced Reggeization of the pion propagator,[3] nor any off-mass-shell dependence, nor lower-lying trajectories in the πN amplutide. To Eq. (2.1) must be added the contribution of the vector-meson-exchange graph[6] of Fig. 1(b).

We are interested in the $J^P = 1^+$ S-wave projection (in the final $\rho\pi$ system) of the Deck amplitude, with t-channel helicity $\lambda_t = 0$. The resulting expression is straightforward to obtain.[3,6] At fixed s, it depends on the momentum transfer t_1 and on the invariant mass M of $\rho\pi$. Among its important properties, we note the following:

(a) In the limit of forward production ($t_1 \to 0$), at large values of s, the $J^P = 1^+$ S-wave $\lambda_t = 0$ projection of Eq. (2.1),

$$T_{J^P=1^+}(M^2, s, t_1),$$

takes on a very simple form,[3]

$$T_{J^P=1^+}(M^2, s, 0) = \alpha \frac{is}{M^2 - m_\pi^2}, \tag{2.2}$$

where α is a known constant, discussed below in subsection C.

(b) For $t_1 \neq 0$, the S-wave projection of Eq. (2.1) exhibits a mass-slope dependence which can be represented to a good approximation as[6]

$$T_{J^P=1^+}(M^2, s, t_1) \cong T_{J^P=1^+}(M^2, s, 0) e^{(1/2)\lambda(M^2)t_1}. \tag{2.3}$$

As we shall see presently, this mass-slope correlation is of practical importance when theoretical results are compared with the experimental spectra. We remark that the mass-slope correlation observed experimentally[2] is in agreement with the predictions of the Deck model.[6] Between $M = 0.9$ and 1.5 GeV, an acceptable parametrization of $\lambda(M^2)$ is (all units in GeV)

$$\lambda(M^2) \simeq -2 + 16/M^2. \tag{2.4}$$

In the next subsection, we discuss certain practical considerations which are important for confrontations with data. Formal theorists and other readers not actually concerned with such detail may skip to subsection C.

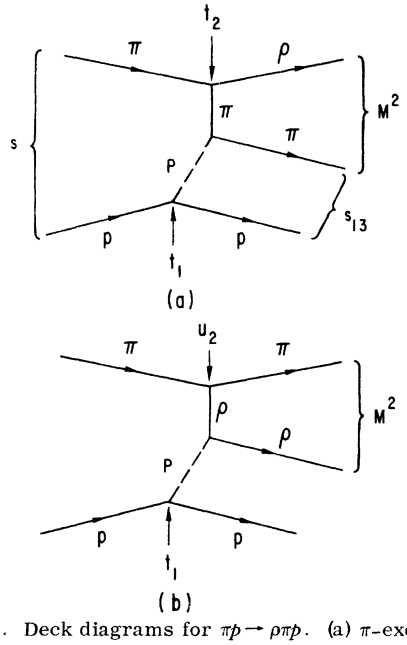

FIG. 1. Deck diagrams for $\pi p \to \rho\pi p$. (a) π-exchange graph, (b) ρ-exchange graph. P stands for Pomeron exchange. The kinematic variables are indicated.

B. Mass-slope correlations and fits to experimental spectra

For analytical convenience [see Eq. (2.2)], and to avoid the introduction of parameters which might obscure the results, we choose to compute amplitudes at $t_1 = 0$. However, the data[2] consist of cross sections integrated over some limited range in t_1, which does not reach $t_1 = 0$. For theoretical purposes, it would obviously be preferable to compare with data extrapolated to $t_1 = 0$. Present statistical precision apparently does not permit a reliable extrapolation.

A second possibility, which we adopt, is to integrate the cross section obtained from Eq. (2.3) over the experimental t_1 range, i.e., to compute

$$\frac{\bar{d}\sigma}{dM} = \frac{d\sigma}{dM dt_1}(t_1 = 0) \int_{t_1'}^{t_1''} e^{\lambda(M^2)t_1} dt_1 = \frac{d\sigma}{dM dt_1}(t_1 = 0) \frac{e^{\lambda(M^2)t_1'} - e^{\lambda(M^2)t_1''}}{\lambda}. \tag{2.5}$$

Since $\lambda(M^2)$ decreases by a factor of ~2 between $M = 1.0$ and 1.4 GeV, Eq. (2.5) shows that *observed* spectra (which correspond typically to $t_1' \sim -0.1$ GeV^2 and $t_1'' \sim -0.3$ GeV^2)^2 will be depleted at low masses when compared to the $t_1 = 0$ Deck model In our opinion, this is a relevant observation for our present A_1 calculation as well as for similar approaches, as in the case of the Q problem.[4] The apparent discrepancy between theory and experiment at low values of M is perhaps mainly due to the fact that the influence of the mass-slope correlation has not been fully appreciated.

We shall use Eq. (2.5) in comparing our results with experiment. However, we emphasize that Eq. (2.3) taken at face value would not be an appropriate expression for the dispersion-relation calculations done in Sec. III. Because of its awkward analyticity properties in M^2, Eq. (2.3) cannot be used as it stands. It is only valid in a limited range in M^2. A fully rigorous treatment for $|t_1| > 0$ would consist in calculating first the true partial-wave projection of Eq. (2.1) for $|t_1| > 0$ [which would be close but not identical to Eq. (2.3)], and then performing the t_1 integration after the dispersion-relation calculation. At the present level of experimental accuracy, we believe that this is an unnecessary complication. We are not concerned with effects which could have a 20 to 30% influence on the results. Our aim is to extract the main qualitative and quantitative aspects within the simplest possible framework.

We shall therefore work at $t_1 = 0$ and apply the dispersion relations rigorously to $T(M^2, s, 0)$, ignoring the M^2 dependence of $e^{(1/2)\lambda(M^2)t_1}$. We then use Eq. (2.5) to compare with the data. A possible *a posteriori* justification stems from the experimental results themselves. Indeed, the data show a mass-slope correlation. By fitting the data to obtain the resulting parameter $\lambda(M^2)$ [which agrees with Eq. (2.4)] and assuming that, for the *physical* amplitude, Eq. (2.5) is correct in the M^2 range of interest, one can invert this latter equation to extract the value of $d\sigma/dMdt_1$ at $t_1 = 0$. This amounts to doing a simple extrapolation to $t_1 = 0$.

C. Specific Deck amplitudes

We choose to work with the simplest and most transparent Deck amplitude. It is clear that improvements can be made, but our main ambition here is to exhibit the essential features of unitarity (or final-state-interaction) corrections to such an amplitude. We feel that given present statistics, it is inappropriate to introduce too many refinements and parameters. However, one essential feature of our approach is the inclusion of channels other than the "elastic" $\rho\pi$ channel. A glance at

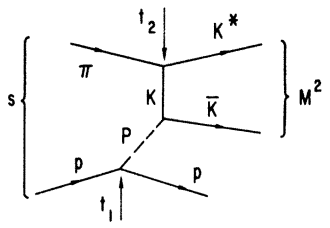

FIG. 2. Kaon-exchange Deck diagram for $\pi p \to K^*\bar{K}p$.

SU(3) coupling coefficients shows that the A_1 state may be strongly coupled to the $K^*\bar{K}$ channel, as well as to $\rho\pi$. While neglect of $K^*\bar{K}$ is understandable if the A_1 is a narrow resonance with mass ~1.1 GeV, the same is not true for a potentially broad resonance with higher mass.

In this article we provide a coupled-channel treatment of the $\pi N \to \rho\pi N$, $\pi N \to K^*\bar{K}N$, and $\pi N \to \bar{K}^*KN$ amplitudes. As remarked in subsection B, we specialize to forward production ($t_1 \to 0$), whereupon simple analytic forms for the $J^P = 1^+$ S-wave $\rho\pi$ and $K^*\bar{K}$ Deck amplitudes are easily obtained[3] from the complete amplitudes for Figs. 1(a) and 2. These $J^{PC} = 1^{++}$ Deck amplitudes with isospin $I = 1$ and t-channel helicity $\lambda_t = 0$ are.[3,6]

$$T_D^{J^P=1^+}(M^2, s, 0) \equiv \begin{bmatrix} T_{\text{Deck}}\ (\rho\pi) \\ T_{\text{Deck}}(K^*\bar{K}) \end{bmatrix}$$

$$= \frac{2i\sqrt{2}\ s}{(M^2 - m_\pi^2)} \begin{bmatrix} g_{\rho^0\pi^+\pi^-} K_\rho \sigma_{\pi p} N_\pi \\ g_{K^{*0}K^+\pi^-} K_{K^*} \sigma_{Kp} N_K \end{bmatrix}. \tag{2.3}$$

We have written the amplitude as a two-component vector to emphasize the two-channel nature of our problem. The mass dependence $(M^2 - m_\pi^2)^{-1}$ is common to the two channels. The upper element of Eq. (2.6) refers to the $\rho\pi$ system with $I = 1$ (thus the $\sqrt{2}$ factor). The lower element refers to the $I = 1$, $C = +1$ combination $(\sqrt{2})^{-1}(K^*\bar{K} - \bar{K}^*K)$ (not just $K^*\bar{K}$ alone). For notational simplicity, we use $K^*\bar{K}$ in the remainder of this paper to represent the $C = +1$ combination. The established coupling constants are $g^2_{\rho^0\pi^+\pi^-} = 4\pi(2.4)$ and $g^2_{K^{*0}K^+\pi^-} = 4\pi(1.66)$; $\sigma_{\pi p}$ and σ_{Kp} are the πp and Kp total cross sections, 24 and 19 mb, respectively, and K_ρ (K_{K^*}) is the magnitude of the incident π momentum evaluated in the $\rho(K^*)$ rest frame at $t_2 = 0$.[6]

We comment briefly here on the normalization constants N_π and N_K in Eq. (2.6), for two reasons. First, the relative normalization of the $\rho\pi$ and $K^*\bar{K}$ Deck terms plays a role in determining the final parameters of our A_1 resonance. Second, as a result of including the A_1 resonance and final-state interactions, we enhance the cross section

in the $\rho\pi$ and $K^*\bar{K}$ channels. Since the cross section from Deck alone[6] is within a factor of 2 or 3 of reproducing the $\rho\pi$ data at 40 GeV/c, only an enhancement factor of this size is permissible.

In the limit of exact SU(3), the $\rho\pi$ and $(\sqrt{2})^{-1}(K^*\bar{K} - \bar{K}^*K)$ Deck amplitudes in Eq. (2.6) are in the ratio $g_{\rho^0\pi^+\pi^-}/g_{K^{*0}K^+\pi^-} \to \sqrt{2}$. This ratio is altered (increased) in practice because $m_K > m_\pi$, $\sigma_{\pi p} > \sigma_{Kp}$, and so forth. In the Deck amplitudes sketched in Figs. 1(a) and 2, form factors of the type $\exp(t_2 - m_\pi^2)$ and $\exp(t_2 - m_K^2)$ are present.[6] One of their effects is to reduce the size of the $J^P = 1^+$ waves; thus, $N_K < N_\pi < 1$ in Eq. (2.6). However, addition of the vector-exchange Deck graphs such as Fig. 1(b) compensates in part[6] for these reductions. After a detailed numerical analysis we find that the properly normalized $J^P = 1^+$ Deck background amplitudes with $\lambda_t = 0$ are obtained if we set $N_\pi \simeq 1$ and $N_K \simeq 0.5$ in Eq. (2.6). Reasonable modifications of these Deck amplitudes do not change any of our major conclusions.

D. Normalized cross sections

To obtain the $J^P = 1^+$ S-wave part of the differential cross section for $\pi^- p \to (\rho^0\pi^-)p$, we must integrate the upper element of Eq. (2.6) over phase space. Including all factors, we derive

$$\left.\frac{d\sigma}{dt_1 dM}\right|_{t_1=0} = \frac{1}{2}\,\frac{1}{0.3893}\,\frac{q_{p\pi}}{8(2\pi)^3 s^2}\left|T_{\text{Deck}}(\rho\pi)\right|^2 \tag{2.7}$$

In Eq. (2.7), $q_{p\pi}$ is the magnitude of the three/vector momentum of the ρ in the $\rho\pi$ rest frame. The factor 0.3893 converts the cross section to mb, under the assumption here that the πp total cross section $\sigma_{\pi p}$ which appears in $T_{\text{Deck}}(\rho\pi)$ is expressed in mb (not GeV) units. The factor of $\frac{1}{2}$ on the right side of Eq. (2.7) is an isospin factor which arises because we present cross sections for the specific change configuration $\pi^- p \to (\rho^0\pi^-)p$.

For the $J^P = 1^+$ S-wave component of the specific reaction $\pi^- p \to (K^{*0}K^-)p$, or $\pi^+ p \to (\bar{K}^{*0}K^+)p$, we derive

$$\left.\frac{d\sigma}{dt_1 dM}\right|_{t_1=0} = \frac{1}{2}\,\frac{1}{0.3893}\,\frac{q_{K^*\bar{K}}}{8(2\pi)^3 s^2}\left|T_{\text{Deck}}(K^*\bar{K})\right|^2. \tag{2.8}$$

In Eq. (2.8), $q_{K^*\bar{K}}$ is the magnitude of the three-vector momentum of the K^* in the $K^*\bar{K}$ rest frame.

III. UNITARITY

A. Formal framework

We impose unitarity by requiring that our amplitude $T_{JP=1^+}(M^2, s, t_1)$, which we denote $T(M^2)$, satisfy the proper discontinuity relation in the variable M^2. We make the usual assumption that we can treat the variable M^2 separately, and that there are no other unitarity corrections, for instance, in the variable s. This is justified by the fact that the reaction takes place at high values of s. We study the amplitude for $\pi p \to (\rho\pi)p$ at low values of $M_{\rho\pi}{}^2$, where πN or ρN rescattering corrections are negligible.

We follow the method of Ref. 5. In the unitarity relation we retain the two-particle intermediate states ($\pi\rho$ and also e.g. $K^*\bar{K}$, $\rho\omega$, etc.), treating the vector mesons as stable, and restricting ourselves to *S-wave* orbital angular momentum states. It is a minor technical problem to extend this procedure to other two-particle states.[5] The three-or-more-particle sector is not easily tractable at present. Considering for generality n communicating intermediate states, we introduce the n-dimensional column vector $T(M^2) \equiv (T_i(M^2) i = 1, n)$ formed of the n amplitudes for producing these states. Apart from other singularities, the amplitude $T(M^2)$ in a given partial wave has a right-hand unitarity cut in M^2 beginning at the lowest threshold $M_R = m_\rho + m_\pi$. Let T^+ and T^- be the values of T above and below this cut, and let $f_l(M^2)$ be the $(n \times n)$ strong-interaction t matrix for this set of states. That is, $f_l(M^2)$ describes the scattering of, e.g., $\rho\pi \to \rho\pi$, $\rho\pi \to K^*\bar{K}$, $K^*\bar{K} \to K^*\bar{K}$, $\rho\pi \to \rho\omega$, etc. For the moment, let us assume that f_l is known. Actually, it is the unknown of our problem. Below, in Sec. IIIB, we will parametrize it in terms of a K matrix.

The unitarity relation for T can be written as

$$(T^+ - T^-)/2i = f_l \rho T^-, \tag{3.1}$$

where ρ is the diagonal phase-space matrix $\rho_{ii} = (2q_i/M)\theta(M^2 - s_i)$; q_i is the c.m. momentum, and s_i is the physical threshold for channel i. Equation (3.1) can be reexpressed as

$$T^+ = ST^-. \tag{3.2}$$

The operator S is

$$S = 1 + 2i f_l \rho. \tag{3.3}$$

It satisfies $SS^* = 1$ (S^* is the complex conjugate of S), if time-reversal invariance holds, and if f_l is symmetric. S is trivially related to the symmetric, unitary strong-interaction $\mathcal{S}$ matrix

$$\mathcal{S} = 1 + 2i\rho^{1/2} f_l \rho^{1/2}. \tag{3.4}$$

Our Eq. (3.2) is the generalized version of Watson's theorem[7] and has been quite thoroughly discussed in Ref. 5. We recall that (a) below the inelastic thresholds (one-channel situation), $T(M^2)$ has the form $\tilde{T}e^{i\delta(M)}$, where $\delta(M)$ is the phase shift for $\pi\rho$ elastic scattering, and (b) above the inelas-

tic thresholds (several intermediate states), unitarity alone does not fix the phases of the production amplitudes. It only provides constraints which relate these phases to each other and to the moduli of the amplitudes, once the two-particle (e.g. $\rho\pi \to \rho\pi$) strong-interaction phases and inelasticities are given.[5]

The final complete unitary partial-wave amplitude $T(M^2)$ has two parts. The first may be termed a unitarized Deck production amplitude and is discussed below in subsection A 1. The second encompasses additional contributions including possible "direct production" of the A_1 resonance, as we explain in subsection A 2.

1. Unitarized Deck amplitude

We construct the unitarized Deck amplitude from a knowledge of its singularity structure, using the Cauchy integral theorem. There are two types of singularities. The discontinuity across the right-hand unitarity cut was described just above. Second, we assume that the "left-hand" singularities of $T(M^2)$ are provided by the production model. These singularities arise from the singularities in t_2 (and u_2) of Figs. 1 and 2. The dominant ones are assumed to be the pion- and ρ-exchange Deck graphs and their sum is therefore by definition $T_D(M^2) \equiv T_{\text{Deck}}$. The problem we address here is the following: Given T_{Deck} and a parametrization of the $J^P = 1^+$ S matrix for, e.g., $\rho\pi$ and $K^*\bar{K}$ scattering, determine an analytic and unitarity amplitude T_D^u with the proper discontinuity structure. The general formal solution of our problem is well known.[5,8] It is first necessary to devise a 2×2 analytic matrix $D(M^2)$ which possesses only the right-hand unitarity discontinuity, satisfying the equation $D^+(M^2) = SD^-(M^2)$, but which is also invertible (viz., the determinant of D should not vanish anywhere on the first sheet). By construction, the function $D^{-1}[T_D^u - T_D]$ then has only a right-hand discontinuity given by $-\text{disc}(D^{-1})T_D$. Writing a dispersion integral for $D^{-1}(T_D^u - T_D)$, we derive as our answer

$$T_D^u(M^2) = T_D(M^2) - \frac{1}{2i\pi} D(M^2) \int_{M_R^2}^{\infty} ds' \frac{\text{disc}(D^{-1}(s'))T_D(s')}{(s' - M^2)} . \tag{3.5}$$

Equation (3.5) is our *definition of the unitarized Deck amplitude*, i.e., the Deck amplitude with rescattering corrections taken into account. The amplitude $T_D^u(M^2)$ has, in particular, the following properties:

(a) It has the same left-hand production model singularities as $T_D(M^2)$.

(b) It satisfies the unitarity relation (3.2).

(c) It reduces to $T_D(M^2)$ if the strong-interaction pseudoscalar vector $\rho\pi$ and $K^*\bar{K}$ scattering amplitudes f_l vanish, in which case $D = 1$ and $\text{Im}\, D = 0$.

In reality the f_l never vanish, but they are presumably negligible for exotic channels such as $\rho^+\pi^+$.

Equation (3.5) is not in general the only amplitude which satisfies the above three requirements. There is a well known polynomial ambiguity[5] when resonances are present. In the Appendix, we give a brief justification for our definition of Eq. (3.5) as the unitarized production amplitude. This choice can be proved more rigorously[9] in nonrelativistic quantum mechanics. In a previous paper,[4] we used an integral over the left-hand cut to obtain our unitarized production amplitude, rather than the integral over the right-hand cut in Eq. (3.5). However, as we remarked, for the choice of parameters required by the Q data analyzed in Ref. 5, this difference has no practical consequences for the Q problem. We now judge that Eq. (3.5) is the correct procedure.

A. Additional contributions

In most of our calculations, the S matrix contains an A_1 resonance, and the D matrix has elements which decrease like powers of M^2, as M^2 approaches infinity. In such cases, an amplitude which satisfies the above criteria (a), (b), and (c), and vanishes at infinity, has the form[5]

$$T(M^2) = T_D^u(M^2) + D(M^2)P(M^2) , \tag{3.6}$$

where $P(M^2)$ is a vector whose n components are polynomials in M^2 and which are such that DP vanishes at infinity. The choice (3.5) is such that $T(M^2) \to T_D(M^2)$ as $M^2 \to \infty$.

We shall argue below that part of the additional contribution DP in Eq. (3.6) can be viewed as a "direct" production of the A_1 resonance. It can also represent the contribution of singularities which may have been omitted in T_{Deck}, are located farther away in M^2, and provide a smooth contribution (apart from unitarity effects) in the M^2 region of interest. For instance, it is clear that our scheme does not explicitly incorporate crossing symmetry, in the sense that unitarity is neglected in the crossed channels t_2 and u_2, where only the poles are taken into account. In order to achieve quantitative agreement with the data, it may be necessary to include the extra term on the right-hand side of Eq. (3.6).

B. Practical method: Basic features of the amplitudes

There are many ways to parametrize the coupled-channel S matrix of interest to us. Even-

tually, given enough data, one will be able to adopt a parametrization in terms of phase shifts and then to determine these by a direct fit to experimental results. Since this desirable level of precision is still some years away for three-particle processes, we adopt instead a simple pole parametrization of S, using a K matrix formalism. As pointed out in Ref. 5 this has the advantage of yielding analytic expressions for the D matrices which we need.

We begin with a real symmetric $n \times n$ K matrix. The S operator of Eqs. (3.2) and (3.3) is then

$$S(M^2) = [1 - K(M^2)C^+(M^2)]^{-1}[1 - K(M^2)C^-(M^2)]. \tag{3.7}$$

In most of what follows, we set $n = 2$, i.e., we shall consider the coupled $\rho\pi$ and $K^*\overline{K}$ channels. The C matrix in Eq. (3.7) is diagonal, $C_{ij} = \delta_{ij}C_i$. The C_i are the usual unequal-mass Chew-Mandelstam functions for $\rho\pi$ and $K^*\overline{K}$. E.g., $C_1(M^2)$ is cut from $M^2 = (m_\rho + m_\pi)^2$ to $+\infty$; for $M > (M_\rho + m_\pi)$, it satisfies $\mathrm{Im}C_1(M^2) = 2q/M$. Each C_i is defined so that $C_i(0) = 0$. Explicitly,

$$C_1(x) = -\frac{2}{\pi}\left\{-\frac{1}{x}[(m_\rho + m_\pi)^2 - x]^{1/2}[(m_\rho - m_\pi)^2 - x]^{1/2} \ln \frac{[(m_\rho + m_\pi)^2 - x]^{1/2} + [(m_\rho - m_\pi)^2 - x]^{1/2}}{2(m_\rho m_\pi)^{1/2}} + \frac{m_\rho^2 - m_\pi^2}{2x} \ln \frac{m_\rho}{m_\pi} - \frac{m_\rho^2 + m_\pi^2}{2(m_\rho^2 - m_\pi^2)} \ln \frac{m_\rho}{m_\pi} - \tfrac{1}{2}\right\}. \tag{3.8}$$

1. One-channel case

As a point of departure and to have a basis for comparison, it is of interest to recall first the main features of the well-known one-channel case. Setting $K = g^2/(s_1 - M^2)$, we obtain

$$D(M^2) = \frac{1}{s_1 - M^2 - g^2 C_1(M^2)}. \tag{3.9}$$

This is a very simple parametrization of a resonant amplitude. For a narrow resonance of mass m and width Γ, the parameters s_1 and g^2 are fixed by $s_1 \simeq m^2 + g^2 \mathrm{Re}C_1(m^2) \simeq m^2$ and $g^2 \mathrm{Im}C_1(m^2) \simeq m\Gamma$. The parameters s_1 and g^2 can be fixed rigorously by imposing the presence of a pole of $D(M^2)$ on the second sheet. This is the manner in which we proceed below. Assuming the simplified form of Eq. (2.2) for the Deck amplitude

$$T_D(M^2) = \frac{\alpha}{M^2 - s_0}, \tag{3.10}$$

we use Eq. (3.5) to obtain the unitarized Deck amplitude. It is

$$T_D^u(M^2) = \frac{\alpha}{M^2 - s_0} \frac{s_1 - M^2 - g^2 C_1(s_0)}{s_1 - M^2 - g^2 C_1(M^2)} \tag{3.11}$$

Since $C_1(s_0)$ is real, this amplitude has a real zero near $M^2 = s_1$. For a narrow resonance, the zero occurs near the resonance mass value, $M^2 = m^2$, as expected (see the Appendix). Thus, the unitarized production amplitude changes sign near the resonance position, and the phase of T_D^u will jump by π. If we now add, as in Eq. (3.6), a "direct production" term

$$D(M^2)\beta = \frac{\beta}{s_1 - M^2 - g^2 C_1(M^2)}, \tag{3.12}$$

where β is a constant, the resulting amplitude $T(M^2) = T_D^u(M^2) + \beta D(M^2)$ has its zero shifted. The new position is

$$M^2 = \frac{\alpha[s_1 - g^2 C_1(s_0)] - \beta s_0}{\alpha - \beta}.$$

This shift of the position of the zero is accompanied by an increased enhancement of the amplitude compared to the Deck amplitude; e.g. for $\beta = \alpha$ the zero is at infinity, and the modulus of the amplitude at the resonance is enhanced by a factor of order m/Γ. Notice, however, that if $\alpha \gg \beta$, then the resonance produces a pronounced *dip* in $d\sigma/dM$ near the nominal resonance location, not a peak.

Because $\cos\delta$ vanishes near $M^2 = s_1$, the M dependence of Eq. (3.11) may be approximated very crudely as $e^{i\delta}\cos\delta$, if the resonance is narrow [i.e., for $g^2 C_1(M^2)$ small]. Even for a broad resonance, the net effect of the zero is significant and causes sharp structure in $d\sigma/dM$ near the resonance position. In our A_1 problem, this effect will explain the steep decrease of the $\rho\pi$ mass distribution in the $J^P = 1^+$ wave near $M = 1.3$ GeV, an effect not obtainable from the pure Deck amplitudes. Stated otherwise, the steep decrease observed in $d\sigma/dM$ helps to fix our parameter s_1, which is related to the position of the A_1 resonance.

Turning now to our specific case of a diffractive process, with the A_1 resonance in the $\pi\rho$ system, we have $\alpha = 2i\sqrt{2}\, s g_{\rho^0\pi^+\pi^-} K_\rho \sigma_{\pi p} N_\pi$, and $s_0 = m_\pi^2$. Our Eq. (3.11) then represents the full physical situation if the A_1 is observed only through the Deck final-state-interaction mechanism. However, once a resonance is postulated, a direct production term may also be present, as is illustrated in Fig. 3.

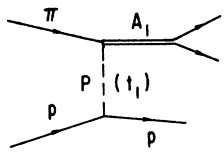

FIG. 3. Diagram representing a direct coupling of the postulated A_1 resonance to the exchanged Pomeron.

The corresponding direct diffractive amplitude is

$$T_{\rm dir}(s,M^2,t_1)=\frac{is\sigma_{\pi p}Gf(t_1)}{s_1-M^2-g^2C_1(M^2)}. \tag{3.13}$$

We omit possible Regge exchange terms proportional to s^{α_R}, $\alpha_R\sim\frac{1}{2}$. Equation (3.13) may be compared to Eq. (3.12). The fact that their analytic forms are identical is our reason for associating Eq. (3.12) with a direct production amplitude. In Eq. (3.13) G is related to the direct πA_1 Pomeron coupling strength, and $f(t)$ represents the t dependence of the Pomeron exchange in Fig. 3. Both are *a priori* unknown and must be determined by fits to data. In particular, $f(t)$ may be different from the t dependence of the unitarized Deck amplitude Eq. (3.11). If the resonance width is narrow, the behavior of Eq. (3.13) as a function of M is roughly that of a Breit-Wigner form, i.e., $\sim e^{i\delta}\sin\delta$. This may be contrasted with the behavior of Eq. (3.11), which, as we remarked, is closer to $e^{i\delta}\cos\delta$. In our comparisons with data, we determine that the direct coupling term Eq. (3.13) plays only a small role in the diffractive A_1 situation.

The structure of our final amplitude for $\pi p \to$ "A_1"p has several features in common with those found in empirical analyses[10] of $\gamma p\to\rho p$. In ρ photoproduction, both a direct diagram (vector dominance) and a Drell-Deck background are implicated. Fits to the data show that the direct diagram is dominant in $\gamma p\to\rho p$, in contrast to our A_1 conclusions, but the unitarized Drell-Deck term nevertheless plays an important role in shifting the ρ to lower mass and in altering its apparent width.[10] We view this example of $\gamma p\to\rho p$ as supporting evidence that our present proposal for the analysis of the A_1 channel has more general applicability. In particular, we consider the $\gamma p\to\rho p$ results as an excellent experimental justification for choosing Eq. (3.5) as the definition of the unitarized Deck amplitude.

We conclude this somewhat pedagogical subsection with some comments about our choice of the strong-interaction amplitude and the D function Eq. (3.9). It is clear that the resonance in our parametrization corresponds to a Castillejo-Dalitz-Dyson (CDD) pole. It is an unstable state coupled to the $\rho\pi$ continuum, and not a dynamical $\rho\pi$ effect. In making this choice, we comply with (a) the experimental observation that phase shifts do not seem to obey Levinson's theorem (do not decrease to zero above the resonance region) and with (b) the present theoretical point of view that meson resonances are primarily $q\bar{q}$ bound states. We could improve our strong-interaction amplitude by taking into account some $\pi\rho$ forces. This can be done easily in an N/D formalism. By choosing

$$N=\sum_i\frac{\alpha_i}{M^2-s_i},$$

and imposing the presence of a CDD pole, we would have

$$D(M^2)=\frac{1}{s_1-M^2-\Phi(M^2)},$$

where

$$\Phi(M^2)=\sum_{i\geq 2}\alpha_i\frac{C_1(M^2)-C_1(s_i)}{M^2-s_i}.$$

It is easy to see that the arguments developed above would remain qualitatively unchanged. While several refinements can be thought of, our point of view has been to choose amplitudes which are as simple as possible.

2. *Two-channel case*

Since the A_1 resonance can have a mass close to 1350–1400 MeV, and since we are interested in the region above 1.4 GeV, it is important to incorporate the inelastic $K^*\bar{K}$ channel in the calculation. We use the K matrix

$$K(M^2)=\begin{pmatrix}\frac{g_1^2}{s_1-M^2} & \frac{g_1g_2}{s_1-M^2}\\ \frac{g_1g_2}{s_1-M^2} & \frac{g_2^2}{s_1-M^2}\end{pmatrix}. \tag{3.14}$$

Here s_1 is related to the mass-squared of the A_1 resonance; g_1 and g_2 are the coupling strengths of the A_1 to the $\rho\pi$ and the $(\sqrt{2})^{-1}(K^*\bar{K}-\bar{K}^*K)$ states; $\alpha^2=g_1^2+g_2^2$. SU(3) specifies $g_1/g_2=\sqrt{2}$ for the A_1, which underlines the importance of including the $K^*\bar{K}$ effects in the analysis. From this simple form chosen for K, we derive

$$D(M^2)=\frac{1}{s_1-M^2-g_1^2C_1-g_2^2C_2}\begin{bmatrix}g_1 & -g_2(s_1-M^2-\alpha^2C_2)\\ g_2 & g_1(s_1-M^2-\alpha^2C_1)\end{bmatrix}. \tag{3.15}$$

For the final $J^P = 1^+$ partial-wave amplitude, we use Eq. (3.5) to obtain

$$T_D^u(M^2) = \frac{1}{s_1 - M^2 - g_1^2 C_1(M^2) - g_2^2 C_2(M^2)} \begin{bmatrix} T_D(\rho\pi)[s_1 - M^2 - g_2^2 C_2(M^2) - g_1^2 C_1(m_\pi^2)] \\ \quad + g_1 g_2 T_D(K^*\bar{K})[C_2(M^2) - C_2(m_\pi^2)] \\ T_D(K^*\bar{K})[s_1 - M^2 - g_1^2 C_1(M^2) - g_2^2 C_2(m_\pi^2)] \\ \quad + g_1 g_2 T_D(\rho\pi)[C_1(M^2) - C_1(m_\pi^2)] \end{bmatrix} \tag{3.16}$$

For each of the two channels, our Eq. (3.16) has the appearance of a resonance factor

$$D_0^{-1}(M^2) \equiv [s_1 - M^2 - g_1^2 C_1(M^2) - g_2^2 C_2(M^2)]^{-1}$$

$$\approx e^{i\delta} \sin\delta$$

multiplied by a function which contains a *complex* zero near $M^2 = s_1$. It is important that the zero is now shifted into the complex plane. This permits a more slowly varying phase in the region where the cross section shows a break (dip), as opposed to the one-channel case, where the phase jumps by 180°.

By simple algebraic manipulation, Eq. (3.16) may be recast in a form with the appearance of a sum of amplitudes: Deck ⊕ resonance. However, both are modified by the requirements of unitarity. We observe again that Eq. (3.16) has the desirable properties that $T_D^u(M^2)$ tends to the unmodified $T_{\text{Deck}}(M^2)$ if the resonance is absent ($g_i = 0$), or if $M^2 \to m_\pi^2$, or if $M^2 \to \infty$. We remark also that $T_D^u \equiv T_{\text{Deck}}(M^2)$ if the resonance is orthogonal to the Deck mixture $g_1/g_2 = -T_D(K^*\bar{K})/T_D(\rho\pi)$ [in the exact-SU(3)-symmetric case with $C_1 = C_2$], as found[4] to be the approximate physical situation for the Q_B. For the parallel mixture, where $g_1/g_2 = T_D(\rho\pi)/T_D(K^*\bar{K})$, the two-channel problem reduces to an effective one-channel case, and

$$T_D^u(M^2) = T_D(M^2)\, \frac{s_1 - M^2 - g_1^2 C_1(m_\pi^2) - g_2^2 C_2(m_\pi^2)}{s_1 - M^2 - g_1^2 C_1(M^2) - g_2^2 C_2(M^2)}. \tag{3.17}$$

A direct production term may also be present, as is illustrated in Fig. 3. The corresponding amplitude is similar to Eq. (3.13):

$$T_{\text{dir}}(s, M^2, t_1) = \frac{is\sigma_{\pi p} G f(t_1)}{D_0(M^2)} \begin{pmatrix} g_1 \\ g_2 \end{pmatrix}$$

$$\equiv D(M^2) \begin{pmatrix} \beta \\ 0 \end{pmatrix}. \tag{3.18}$$

3. *Two-channel, two-pole K matrix*

In our investigations, we have also studied a slightly more sophisticated expression than Eq. (3.14) for the K matrix. The reason is primarily to be able to modify the inelasticity independently of the relative coupling of the A_1 to $\rho\pi$ and $K^*\bar{K}$. The $\rho\omega$ channel, for instance, has a threshold at ~1550 MeV, the P-wave $\epsilon\pi$, D-wave $\rho\pi$ channels, etc. are present, and there are other possible inelastic effects which we represent globally by the sole $K^*\bar{K}$ channel. We also want to have more flexibility in our parametrization of the pseudoscalar-vector coupled-channel amplitude, and to be able to incorporate a nonresonant background contribution and/or a second resonance.

A simple two-pole form for the K matrix is

$$K = \begin{pmatrix} \frac{g_1^2}{s_1 - M^2} + \frac{f_1^2}{s_2 - M^2} & \frac{g_1 g_2}{s_1 - M^2} + \frac{f_1 f_2}{s_2 - M^2} \\ \frac{g_1 g_2}{s_1 - M^2} + \frac{f_1 f_2}{s_2 - M^2} & \frac{g_2^2}{s_1 - M^2} + \frac{f_2^2}{s_2 - M^2} \end{pmatrix}. \tag{3.19}$$

The D matrix becomes

$$D = \frac{1}{D_0} \begin{pmatrix} g_1(s_2 - M^2) - C_2(M^2) f_2 \Lambda & f_1(s_1 - M^2) + g_2 C_2(M^2)\Lambda \\ g_2(s_2 - M^2) + C_1(M^2) f_1 \Lambda & f_2(s_1 - M^2) - g_1 C_1(M^2)\Lambda \end{pmatrix}. \tag{3.20}$$

Here $\Lambda = g_1 f_2 - g_2 f_1$ and

$$D_0(M^2) = (s_1 - M^2)(s_2 - M^2) - C_1(M^2)[g_1^2(s_2 - M^2) + f_1^2(s_1 - M^2)]$$
$$- C_2(M^2)[g_2^2(s_2 - M^2) + f_2^2(s_1 - M^2)] + C_1(M^2) C_2(M^2)\Lambda^2. \tag{3.21}$$

As before, we use Eq. (3.5) to obtain $T_D^u(M^2)$. All the necessary integrals may be evaluated analytically again and yield simple, if lengthy, results in closed form. The polynomial $P(M^2)$ of Eq. (3.6) can have the form

$$P(M^2) = is\sigma_{\pi N} \begin{pmatrix} G_1 f_1(t_1) \\ G_2 f_2(t_1) \end{pmatrix}, \tag{3.22}$$

where G_1, G_2, f_1, and f_2 do not depend on M^2. It is clear in this case that the interpretation of the whole term $D(M^2)P(M^2)$ as "direct production" is less straightforward than in the simpler case of Eq. (3.18). Although it does contain direct production of the resonance, additional terms are also included here in DP.

C. Summary

The two-channel two-pole formulation of subsection B 3 includes the previous two examples as special cases, obtained by setting some of the coupling strengths to zero in Eq. (3.19). Our final unitary coupled-channel partial-wave amplitude $T(M^2)$ is expressed by Eq. (3.6). The term $T_D^u(M^2)$ is obtained from Eq. (3.5), with $D(M^2)$produced in Eq. (3.20). At $t=0$, our direct production term $D(M^2)P(M^2)$ is obtained from Eq. (3.20) and

$$P(M^2)\equiv is\sigma_{\pi N}\begin{pmatrix} a \\ b \end{pmatrix}, \tag{3.23}$$

where a and b are adjustable constants. Our parameters are therefore the two g_i, the two f_i, the two s_i, a, and b.

In Sec. IV, we compare spectra computed from $T(M^2)$ with data, using Eqs. (2.7) and (2.8) to compute differential cross sections at $t_1=0$, and Eq. (2.5) for $|t_1|>0$. We also compare phases with available data. We *define* $\phi(1^+)$ to be the phase of $T(M^2)$, after removing the overall 90° production phase represented by i in Eqs. (2.6) and (3.23). Thus, if unitarity effects were negligible and the unmodified Deck amplitude (2.6) alone were the correct answer, then $\phi(1^+)\equiv 0°$ (real, positive). In Sec. IV A, we describe how $\phi(1^+)$ is extracted from the data for comparison with our model calculations.

The phase $\phi(1^+)$ is, of course, the phase of the $J^P=1^+$ S-wave $\rho\pi$ amplitude as observed in $\pi p \to (\rho\pi)p$. It is also interesting to examine the S-wave phase shift δ and the elasticity η parameters which our model provides for $\rho\pi\to\rho\pi$. To obtain these, we note that the diagonal elements of the S operator Eq. (3.3) may be expressed as $\eta e^{2i\delta}$. Therefore, for the $\rho\pi\to\rho\pi$ amplitude, we derive

$$\frac{\eta e^{2i\delta}-1}{2i}=\frac{2q_{\rho\pi}}{M}\frac{g_1^2(s_2-M^2)+f_1^2(s_1-M^2)-\Lambda^2C_2(M^2)}{D_0(M^2)}. \tag{3.24}$$

In Eq. (3.24), $q_{\rho\pi}$ is the magnitude of the three vector momentum of the ρ in the $\rho\pi$ rest frame; $D_0(M^2)$ is defined in Eq. (3.21).

IV. RESULTS AND INTERPRETATION

We have attempted to reproduce three desiderata: (i) the absolute normalization of the $J^P=1^+$ S-wave $\rho\pi$ cross section, (ii) the position and width of the peak observed in the $J^P=1^+$ S-wave $\rho\pi$ intensity, and (iii) the magnitude and slow variation with mass of the experimentally determined phase of this $J^P=1^+$ S wave.

A. Data

1. Normalization and mass dependence

We use symbol $\bar{\sigma}$ to denote the differential cross section $d\sigma/dt_1dM_{\rho\pi}$ averaged between $M=1.0$ and 1.2 GeV and extrapolated to $t_1=0$. For the $J^P=1^+$ S-wave $\rho\pi$ system in the specific charge state $\rho^0\pi^-$ from $\pi^-p\to(\rho^0\pi^-)p$, $\bar{\sigma}$ is experimentally[2] $\bar{\sigma}=4.3\pm0.3$ mb/GeV^3. The data we use are taken from an analysis of $\pi^-p\to(3\pi)^-p$ at 40 GeV/c and are an experimental average over a range of t_1. This average smears both the mass and phase variations. When data on 3π production reach the level of precision available in $\pi p\to(2\pi)N$, one may contemplate extrapolations to $t_1=0$ and/or amplitude analyses at fixed t_1. For now, we compare the experimental mass spectrum with the integral of the square of our model amplitude,

$$\int_{t_1'}^{t_1''}|T(M^2,t_1=0)|^2\exp(\lambda t_1).$$

The slope $\lambda(M)$ is specified by the Deck model.[3,6] As mentioned in Sec. II, we parametrize it as $\lambda(M^2)=-2+16/M^2$. We have chosen $t_1'=-0.1$ GeV^2 and $t_1''=-0.3$ GeV^2. The choice $t_1'=-0.03$ would reinforce our curves slightly for low values of M^2.

2. Phases

In order to obtain the experimental phase of the 1^+ S-wave $\rho\pi$ amplitude, we use the 40-GeV/c data[2] on the mass dependence of the phase difference, $\phi(2^+)-\phi(1^+)$, between the "A_2" and "A_1" $\rho\pi$ partial waves. This difference passes through zero close to the nominal A_2 position $M_{A_2}\simeq 1.32$ GeV. Data from the same experiment have been used to show that the overall energy (s) dependences for production of the A_1 and A_2 waves are essentially identical for $p_{\text{lab}}\gtrsim 10$ GeV/c. According to standard theorems relating phase and energy dependence, this implies that the *production* phases should also be identical.[11] Therefore, we interpret the phase difference as due approximately entirely to the relative *decay* phases of the 2^+ and 1^+ $\rho\pi$ waves. Because the 2^+ amplitude is saturated by the bona fide A_2 resonance, with little background, Deck or otherwise, its phase rises through 90° at M_{A_2} and should head towards 180°. The fact that $\phi_{\text{rel}}\simeq 0$ near M_{A_2} implies that the experimental absolute phase $\phi(1^+)$ is also near 90° for M in the neighborhood of M_{A_2}.

Since the 2^+ wave is free from background,[2] we adopt a standard Breit-Wigner form[12] to describe the 2^+ amplitude:

$$T^{-1}(A_2) \propto M^2 - M_{A_2}{}^2 + iM_{A_2}\Gamma(M)$$

and

$$\Gamma(M) = \Gamma_0 \left(\frac{q}{q_0}\right)^5 \frac{\rho(q)}{\rho(q_0)}$$

with $M_{A_2} = 1.315$ GeV, $\Gamma = 0.115$ GeV, and $\rho(q) = (9 + 3R^2q^2 + R^4q^4)^{-1}$. The q^5 factor ensures the correct threshold behavior. We employ a cutoff factor with radius[12] $R = 4.4$ to guarantee[13] that $\phi(A_2) \to 180°$ for $M \gg M_{A_2}$.

From this 2^+ phase and the experimental difference $\phi(2^+) - \phi(1^+)$ we obtain the 1^+ phase to which we compare our results. Notice, however, that it is possible that the actual values of $\phi(1^+)$ could be systematically lower by 5 to 10° if the production phases for the "A_2" and "A_1" are not strictly equal,[11] or as occurs in a "unitarized" amplitude analysis of the same data.[14]

Other phase differences have been measured[2] in addition to $\phi(2^+) - \phi(1^+)$. Nevertheless, only the 2^+ wave provides what we may term an "absolute reference phase," allowing us to fix within reasonable bounds the value of the 1^+ phase near $M = 1.3$ GeV. Phases of the 1^+ $(\rho\pi)$ wave measured with respect to various $(\epsilon\pi)$ waves are instructive in one additional respect. They show that the mass dependence of the 1^+ $\rho\pi$ wave is most likely rather smooth and slowly varying over the mass range up to ~1.8 GeV. We accept this as a qualitative constraint on our solutions. Because the ϵ is so ill defined, we do not attempt to devise a model for the $(\epsilon\pi)$ waves. Accepting our theoretical determination of the absolute phase of the $J^P = 1^+$ $\rho\pi$ wave, one may use data on various phase differences to deduce the absolute phases of a large set of partial waves, e.g. that of the $J^P = 1^-$ P-wave $\rho\pi$ system.

B. Model solutions

As mentioned in Sec. II, we begin with the very simple Deck amplitude of Eq. (2.6). We are interested in finding what S-matrix parameters for $\rho\pi \to \rho\pi$ can account for the diffractive data, based on the method described in Sec. III. In practice, we select values for the parameters g_i, f_i, and s_i which enter Eq. (3.19) [or Eq. (3.14), to which Eq. (3.19) reduces in the limit where some of the g_i or f_i vanish]. For the "direct production" term of, e.g., Eq. (3.22), we choose the functions $G_1 f_1(t_1)$ and $G_2 f_2(t_1)$ to be constants, and therefore parametrize $P(M^2)$ as

$$P(M^2) = is\sigma_{\pi N}\begin{pmatrix} a \\ b \end{pmatrix}. \tag{4.1}$$

While the t dependences of the direct production and of the Deck amplitudes are in general different, the present data are not sufficiently detailed to warrant our introducing such luxurious complications. In an attempt to elucidate the physics of the problem, we shall not merely present one "best" fit to the data, but we shall display a set of six "solutions" with different characteristics. These solutions, denoted by A, B, C, D, E, F correspond to values of the parameters given in Table I.

A question of particular importance is whether an A_1 resonance can be established. For each solution, we have searched for the presence of second-sheet poles. Since ours is a coupled-channel problem, the complex M^2 plane has a four-sheeted structure. We can classify these four sheets in the standard way according to (sign(Im$q_{\rho\pi}$), sign(Im$q_{K^*\bar{K}}$)). Sheet I = (+, +) is the physical sheet, sheet II = (−, +) is closest to the physical region below the $K^*\bar{K}$ threshold, sheet III = (−, −) is closest above this threshold, and sheet IV is (+, −). In all our solutions, except solution F which corresponds to a nonresonant amplitude, we have found a pole

TABLE I. Values of the parameters for the six solutions described in the text. These parameters are defined in Eqs. (3.19) and (4.1). The asterisk next to some of the values of g_2 indicates that the ratio $g_1/g_2 = \sqrt{2}$, as specified by SU(3) for the A_1.

Parameters	Solution A	B	C	D	E	F
g_1 (GeV)	0.88	0.94	0.85	0.98	1.74	1.7
g_2 (GeV)	0	0.66*	0.60*	0.42	1.23*	1.7
$\sqrt{s_1}$ (GeV)	1.43	1.495	1.48	1.55	1.89	2.0
f_1 (GeV)	0	0	1.27	5.5	7.1×10^2	0
f_2 (GeV)	0	0	2.16	46.7	-6.4×10^2	0
s_2 (GeV^2)	•••	•••	14.4	1.37×10^3	-3.3×10^5	•••
$a/2$	0.47	0.38	0.7	0.25	0.24	0
$b/2$	0	0	−3.2	0	0	0

TABLE II. Physical parameters associated with the six solutions described in the text. M_{A_1} and Γ_{A_1} are the mass and width of the A_1. They are determined from the position of the second-sheet pole. a_0 is the $\pi\rho$ S-wave scattering length in pion Compton wavelengths, and $\bar{\sigma}$ is the average value of $d\sigma/dt_1 dM$ $(t_1=0)$ between $M=1.0$ and 1.2 GeV.

Characteristics \ Solution	A	B	C	D	E	F
M_{A_1} (GeV)	1.360	1.382	1.383	1.485	1.186	...
Γ_{A_1} (GeV)	0.480	0.470	0.425	0.520	0.394	...
$a_0 (m_\pi^{-1})$	0.30	0.31	0.33	0.30	0.02	0.66
$\bar{\sigma}$ (mb/GeV^3)	5.4	5.4	5.1	4.9	4.7 4.3 if $a=0$	4.5

in sheet II. The positions of the poles for the various solutions are given in Table II, together with the values of the averaged cross section $\bar{\sigma}$, and the values of the $\pi\rho$ S-wave scattering length a_0. This latter quantity is of some interest since we may compare it with the Weinberg current-algebra prediction[15] of $a_0 \sim 0.22 m_\pi^{-1}$.

1. *One-channel, one-pole reference model*

Solution A corresponds to a purely elastic, one-channel, $\pi\rho$ amplitude, parametrized with a very simple one-pole K matrix. No inelastic effects are incorporated. It is displayed in Fig. 4. Some direct production is included. This solution is the starting point of our discussion since, in other solutions, we will try to eliminate its defects while maintaining its appealing features. In Fig. 4(c) we show the full differential cross section at $t_1=0$, compared to that from the unmodified $T_{\text{Deck}}(\rho\pi)$ alone, as well as the contribution to the final result from the direct term alone. A few points may be stressed. The sharp decrease of $d\sigma/dM$ between 1.2 and 1.4 GeV arises from the final-state interactions embodied in Eqs. (3.11)—i.e., the zero near $M^2 = s_1$ (discussed above). It is even more pronounced if $a=0$ in Eq. (4.1), i.e., no direct production. This sharp decrease is also seen in the data displayed in Fig. 4(a). It is evidence in our framework for a resonance and helps to fix our parameter s_1. The large peak centered between $M=1.1$ and 1.2 GeV in Figs. 4(a) and 4(c) is not the A_1 resonance. Rather, it is the Deck background enhanced and sharpened by final-state interactions. The peak in $d\sigma/dM$ at $t=0$, which would be observed if there were no Deck background, is that shown for the direct term alone in Fig. 4(c). This broad structure centered near $M=1.35$ GeV may be observed in the $J^P=1^+$ $\rho\pi$ $I=1$ cross section extracted from forward charge- or hypercharge-exchange data [e.g. $\pi^- p \to (3\pi)^0 n$], from $\bar{p}p$ annihilation data, or in neutrino-induced reactions, where the backgrounds should be substantially smaller. Low-energy charge-exchange data[16] are at least qualitatively consistent with this expectation. Higher-energy and much-higher-statistics charge-exchange data should be instructive.

Although the mass spectrum and the averaged cross section agree well with the data, the phase, Fig. 4(b) differs substantially from the data. The unitarized amplitude changes sign owing to the presence of the zero near s_1. Correspondingly, the phase suffers a sudden change of 180° at ~1540 MeV (this value of mass would be lower if we set $a=0$), whereas no evidence for such a change appears in the data. As indicated in Table II. the A_1 resonance is quite broad ($\Gamma \sim 480$ MeV) in this one-pole calculation, but a broad resonance cannot produce a flattening of the $J^P=1^+$ S-wave phase above 1400 MeV. We note that the resonance in this solution turns out to be close to the inelastic $K^*\bar{K}$ threshold. It is apparent physically that we cannot avoid incorporating inelasticity in the calculation, especially if we want to explain the region above 1400 MeV. We note that there are many possible sources of inelasticity; besides $K^*\bar{K}$, there are the $\epsilon\pi, f_0\pi, \rho\omega, \ldots$ channels.

2. *Two-channel, one-pole model*

Solution B, shown in Fig. 5, represents a coupled-channel calculation involving the $\rho\pi$ and $K^*\bar{K}$ intermediate states. The K matrix is again very simple, with a single factorized pole, and a ratio $g_1/g_2 = \sqrt{2}$ in agreement with SU(3) predictions for the A_1. The values of the parameters are provided in Table I. The mass spectrum shown in Fig. 5(a) is again quite acceptable. The resonance position and width (cf. Table II) are essentially the same as in our one-channel reference example. The phase now has a more acceptable behavior up to 1.5 GeV owing to the introduction of inelasticity. It rises slowly at first, passing through 90° near $M=1.36$ GeV, then displays a cusp at the $K^*\bar{K}$ threshold, and flattens off up to 1500 MeV. However, above 1.5 GeV it decreases rapidly toward zero. In con-

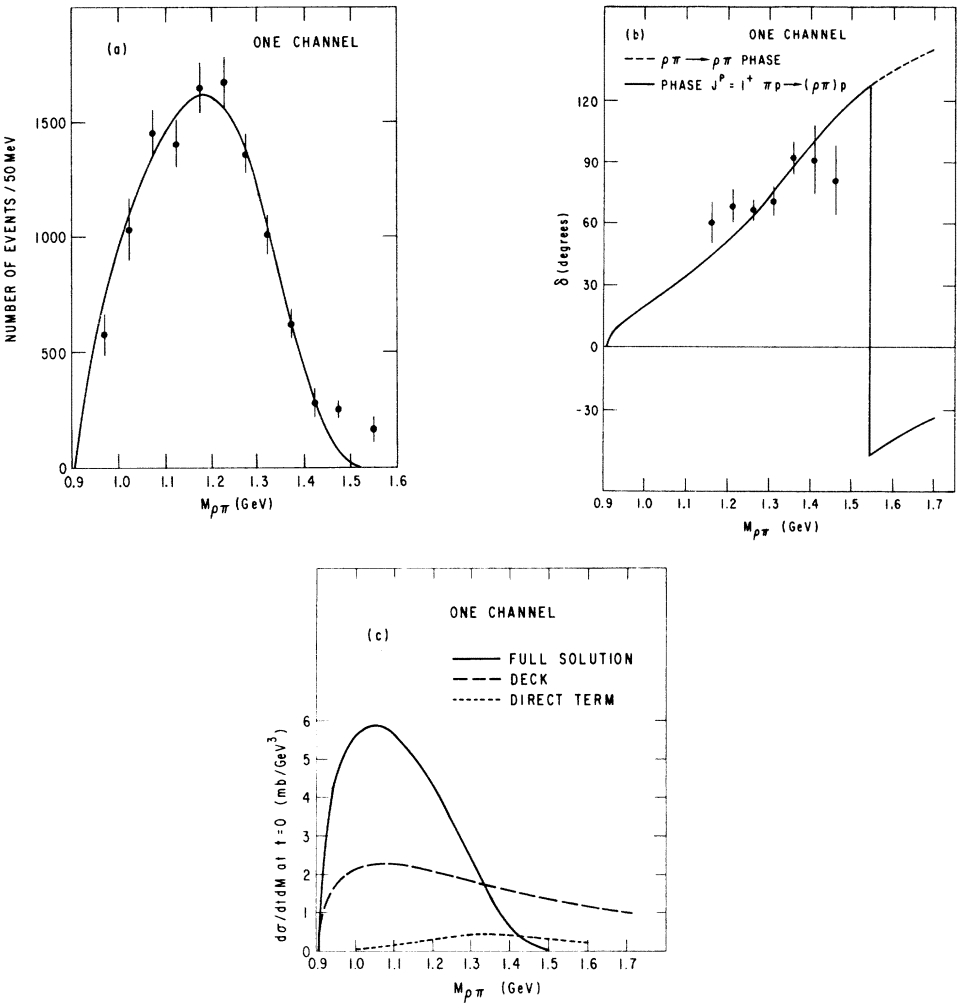

FIG. 4. The naive one-channel, one-resonance model, solution A, described in the text and in Tables I and II. Data points are taken from Ref. 2. The points for the absolute phase of the $J^P = 1^+$ S-wave amplitude in (b) are reconstructed from the experimental difference $\phi(2^+) - \phi(1^+)$, as described in the text. (a) Mass spectrum. The solid line represents our solution A, integrated over $|t|$ from 0.1 to 0.3 GeV^2, as described in the text, and normalized to the data. For absolute normalization and the A_1 resonance parameters, consult Table II. (b) The solid line is the phase of the 1^+ S-wave $\rho\pi$ amplitude in $\pi p \to (\rho\pi)p$; the dotted line is the phase of the $\rho\pi \to \rho\pi$ elastic amplitude in our model. (c) The differential cross section $d\sigma/dt_1 dM$ at $t_1 = 0$ for the specific charge state $\pi^\pm p \to (\rho^0\pi^\pm)p$ at high energy. The solid line represents our full solution; the dashed line is the pure Deck background, without unitarity corrections; the dotted line is the contribution of the direct production term alone.

trast to this rise and fall of the phase of our full diffractive amplitude $T_{\rho\pi}(M^2)$, the phase of the subamplitude for $\rho\pi \to \rho\pi$ is perfectly normal, as shown in Fig. 5(c). Indeed our $\rho\pi \to \rho\pi$ amplitude follows the boundary of the unitarity circle until $M = 1.39$ GeV, whereupon it enters sharply, but continues its rotation with an average elasticity parameter $\eta \simeq 0.7$. The reason for the cusp and for the net overall slow variation of the phase in $\pi p \to (\rho\pi)p$ is the presence of the two channels.

The sharp decrease toward zero at ~1.6 GeV is perhaps one artificial feature of the phase in Fig. 5(b) which does not seem to be present in the data. This decrease is a direct reflection of the change in sign of the unitarized amplitude and of the shift by 180° of the phase of the one-channel solution A. The shift is softened by the inelasticity because the zero of the amplitude now lies in the complex plane. For $M \gtrsim 1.45$ GeV, the intensity of the 1^+ wave is rather small experimentally, and events so identified may in fact be misclassified owing to ambiguities in the partial-wave analysis. It is perhaps not possible to rule out a sign change in $T(M^2)$. Nevertheless, the descent of our calculated

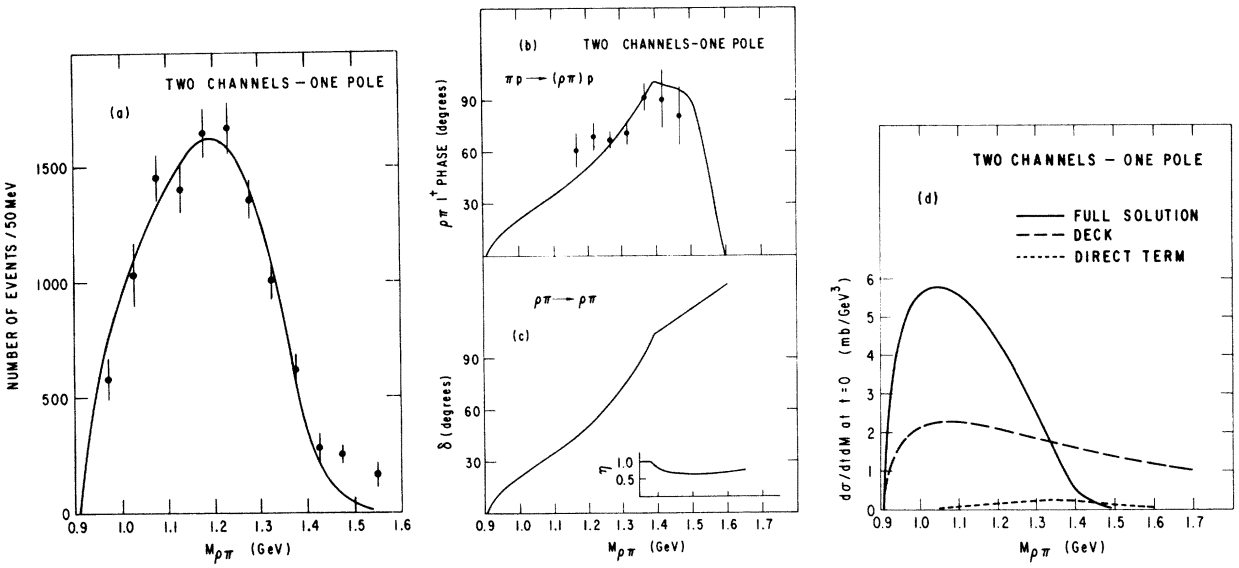

FIG. 5. Two-channel, one-pole model, solution B, described in the text and in Tables I and II. Data points in (a) are taken from Ref. 2. The points for the absolute phase of the $J^P = 1^+$ S-wave amplitude in (b) are reconstructed from the experimental difference $\phi(2^+) - \phi(1^+)$, as described in the text. (a) Mass spectrum. The solid line is our solution B, integrated over the range $|t| = 0.1$ to 0.3 GeV^2, as described in the text, and normalized to the data. For absolute normalization and the A_1 resonance parameters, consult Table II. (b) The phase of our 1^+ S-wave $\rho\pi$ amplitude in $\pi p \to (\rho\pi)p$. (c) The phase-shift and (inset) inelasticity parameters of the $\rho\pi \to \rho\pi$ S-wave amplitude as computed from our model B. (d) The differential cross section $d\sigma/dt_1 dM$ at $t_1 = 0$ for the specific charge state $\pi^\pm p \to (\rho^0\pi^\pm)p$. The solid line represents our full solution B; the dashed line is the pure Deck "background," without unitarity corrections; the dotted line is the contribution of the direct production term alone.

phase $\phi(1^+)$ for $M \gtrsim 1.5$ GeV seems to us unacceptable abrupt. In order to correct for this, a simple and reasonable procedure is to use a $\rho\pi$ and $K^*\overline{K}$ vector-pseudoscalar two-channel S matrix which is more sophisticated than the very simple one-pole K matrices of solutions A and B.

3. *Two-channel, two-pole model*

Solution C, displayed in Fig. 6, corresponds to a two-pole K matrix and a two-component "direct production" term. It is also constructed so as to be very close to solutions A and B as far as $\rho\pi \to \rho\pi$ scattering is concerned, below the inelastic $K^*\overline{K}$ threshold, and to have similar parameters for the A_1 resonance. We notice that (a) the behavior of the phase in Fig. 6(b) is now much smoother and therefore more acceptable, and (b) the mass spectrum also is improved above 1.4 GeV.

From the three solutions A, B, and C, we deduce the following observations:

(1) The elastic $\rho\pi \to \rho\pi$ phase shifts below the $K^*\overline{K}$ threshold are extremely similar in these solutions [cf. Figs. 4(b), 5(c), and 6(c)]. It is this phase shift which really determines the shape of the mass spectrum below $M = 1.4$ GeV. Thus, it is not surprising that the resulting spectra are also similar.

(2) The three solutions differ considerably above 1.4 GeV. These differences are apparent in the $\rho\pi \to \rho\pi$ amplitude and in our amplitude $T(M^2)$. It is clear that inelasticity *must* be introduced in order to yield a flattening of the phase above 1.4 GeV. Furthermore, a sophisticated treatment is required of both the $\rho\pi$ and $K^*\overline{K}$ $2 \rightleftharpoons 2$ coupled amplitude and the "direct production" term, which contains direct production of the resonance and contributions of omitted left-hand singularities in M^2.

(3) It is interesting, however, that the two regions above and below 1.4 GeV seem to be disconnected. We can modify what happens above this energy without changing appreciably what happens below.

(4) The S-wave scattering lengths in these three solutions can be considered in acceptable agreement with the current-algebra prediction, since the predicted value is expected to be increased owing to the presence of a resonance, as in the case of the $I = 0$ S-wave $\pi\pi$ amplitude.

(5) The absolute normalizations at $t_1 = 0$, $\overline{\sigma}$, are somewhat higher (by ~25%) than the experimental value. We do not consider this to be an important flaw. It could be repaired by a reduction of 10% in the absolute normalization of our Deck ampli-

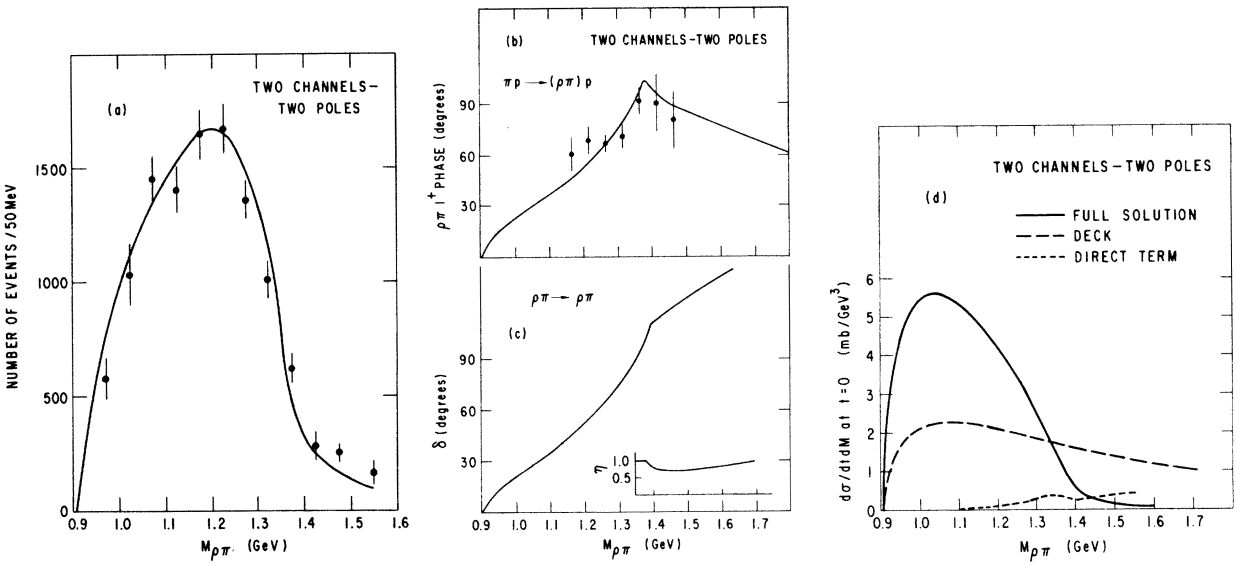

FIG. 6. Two-channel, two-pole model, solution C, described in the text and in Tables I and II. Data points in (a) are taken from Ref. 2. The points for the absolute phase of the $J^P = 1^+$ S-wave amplitude in (b) are reconstructed from the experimental difference $\phi(2^+) - \phi(1^+)$, as described in the text. (a) Mass spectrum. The solid line is our solution C, integrated over the range $|t| = 0.1$ to 0.3 GeV^2, as described in the text, and normalized to the data. For absolute normalization and the A_1 resonance parameters, consult Table II. (b) The phase of our 1^+ S-wave $\rho\pi$ amplitude in $\pi p \to (\rho\pi)p$. (c) The phase-shift and (inset) inelasticity parameters of the $\rho\pi \to \rho\pi$ S-wave amplitude as computed from our model C. (d) The differential cross section $d\sigma/dt_1 dM$ at $t_1 = 0$. The solid line represents our full solution C; the dashed line is the pure Deck "background," without unitarity corrections; the dotted line is the contribution of the direct production term alone.

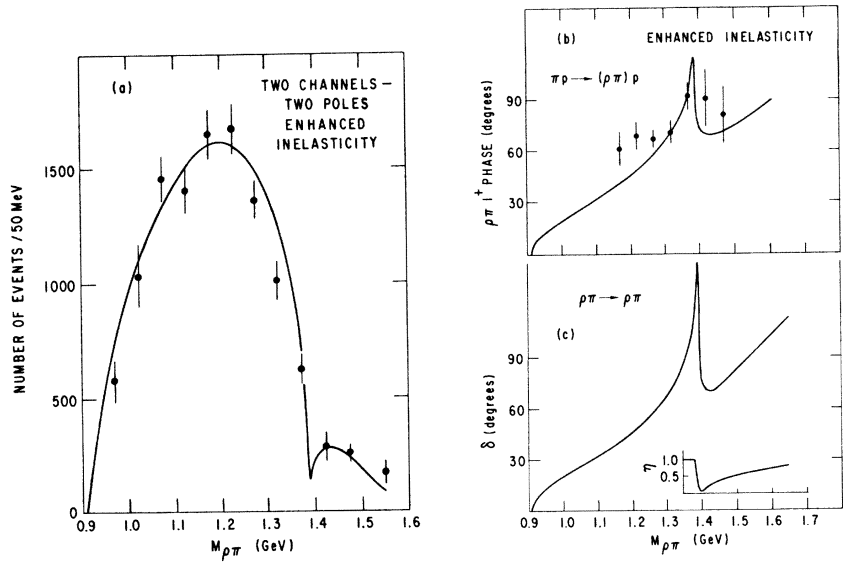

FIG. 7. Two-channel, two-pole model with enhanced inelasticity, solution D, described in the text and in Tables I and II. Data points in (a) are taken from Ref. 2. The points for the absolute phase of the $J^P = 1^+$ S-wave amplitude in (b) are reconstructed from the experimental difference $\phi(2^+) - \phi(1^+)$, as described in the text. (a) Mass spectrum. The solid line is our solution D, integrated over the range $|t| = 0.1$ to 0.3 GeV^2, as described in the text, and normalized to the data. For absolute normalization and the A_1 resonance parameters, consult Table II. (b) The phase of our 1^+ S-wave $\rho\pi$ amplitude in $\pi p \to (\rho\pi)p$. (c) The phase-shift and (inset) inelasticity parameters of the $\rho\pi \to \rho\pi$ S-wave amplitude as computed from our model D.

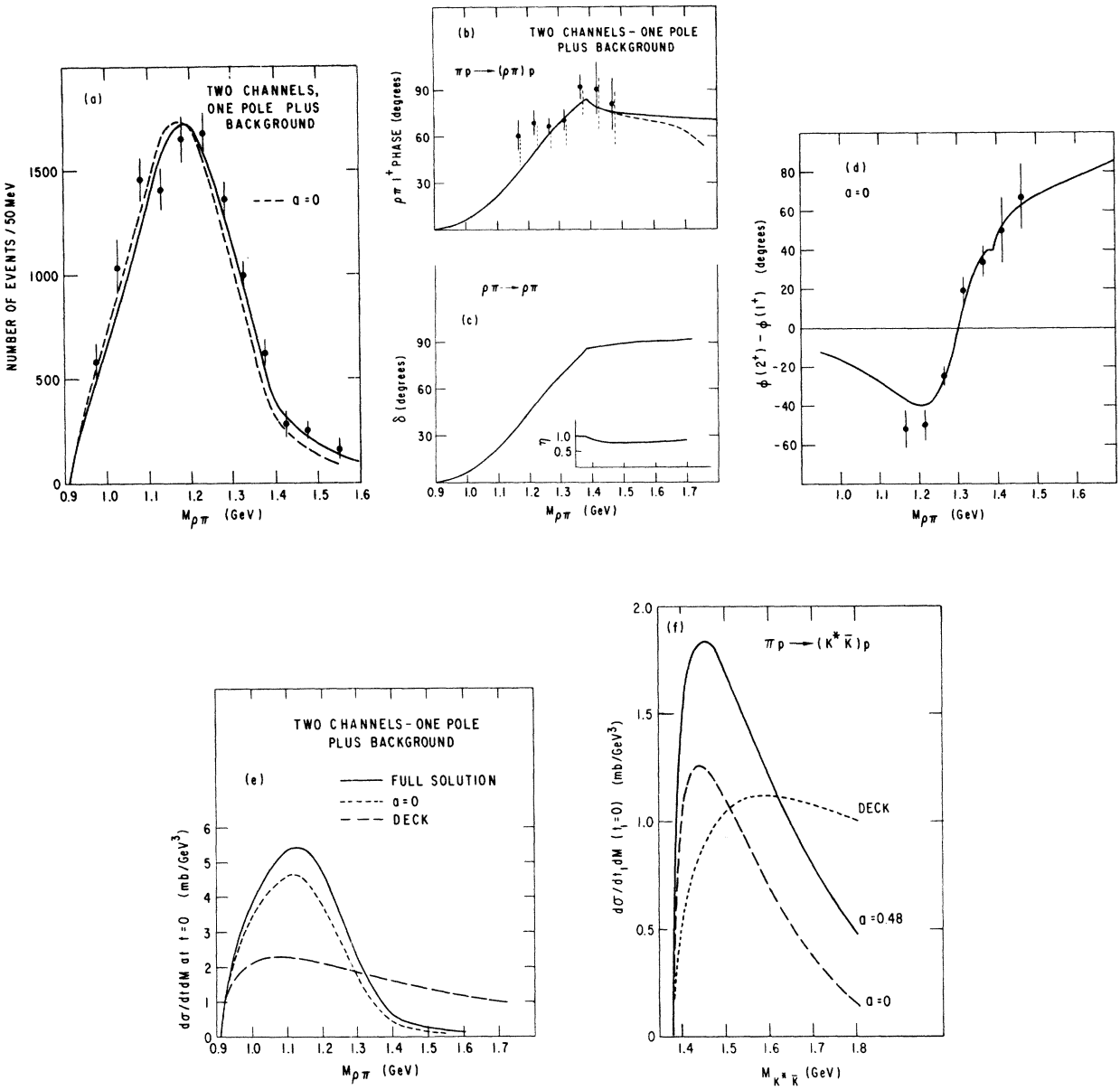

FIG. 8. Two-channel, one-pole model with background in the K matrix, solution E, described in the text and in Tables I and II. Data points in (a) are taken from Ref. 2. The points for the absolute phase of the $J^P = 1^+$ S-wave amplitude in (b) are reconstructed from the experimental difference $\phi(2^+) - \phi(1^+)$, as described in the text. (a) Mass spectrum. The solid line is our solution E, integrated over the range $|t| = 0.1$ to 0.3 GeV^2, as described in the text, and normalized to the data. The dashed curve is obtained by setting $a = 0$— i.e., no direct production. For absolute normalization and the A_1 resonance parameters, consult Table II. (b) The phase of our 1^+ S-wave $\rho\pi$ amplitude in $\pi p \to (\rho\pi)p$. The solid line corresponds to $a = 0.48$. and the dashed line to $a = 0$ (no direct production). The dotted data points are obtained by shifting the solid data points down by 10°, under the assumption of a 10° difference in the production phases of the 2^+ and 1^+ waves. (c) The phase-shift and (inset) inelasticity parameters of the $\rho\pi \to \rho\pi$ S-wave amplitude as computed from our model E. (d) The phase difference $\phi(2^+) - \phi(1^+)$ computed from our model is compared with the data from Ref. 2. Here $a = 0$, and the difference of the *production* phases of the 2^+ and 1^+ waves (cf. Ref. 11) has been assumed to be 10°. (e) The differential cross section $d\sigma/dt_1 dM$ at $t_1 = 0$ for $\rho\pi$ production in the reaction $\pi^- p \to (\rho^0\pi^-)p$. The solid line represents our full solution E, with $a = 0.48$. For the dotted curve, the direct production term is omitted ($a = 0$). The dashed curve is the pure Deck background without unitarity corrections. (f) The differential cross section $d\sigma/dt_1 dM$ at $t_1 = 0$ for $K^*\bar{K}$ production in $\pi^- p \to (K^{*0}K^-)p$. The solid line is our solution E with $a = 0.48$. whereas the dashed curve is obtained by setting $a = 0$ (no direct production). The dotted curve in the pure Deck background without unitarity corrections.

tudes, well within the inherent theoretical uncertainties of the model.

4. Two-channel, two-pole model with enhanced inelasticity

In order to illustrate the effects which important inelasticity can produce, we display solution D in Fig. 7.

In this example, which we consider *academic* by itself but whose results must be kept in mind in view of future calculations, when more abundant data will be available, there is a very strong inelastic effect at the $K^*\bar{K}$ threshold. In Fig. 7(c) the elasticity parameter drops to $\eta = 0.05$ at 1.4 GeV. Notice the behavior of the phase in Fig. 7(b), and also that dip occurs in the mass spectrum in Fig. 7(a) at the opening of the inelastic channel. We present this example because it is not impossible that a similar dip does exist in the data, reflecting the presence of strong inelastic threshold effects.

5. Two-channel, one-pole model with background in the K matrix

Solution E, shown in Fig. 8, is the one which fits the experimental results best. It is constructed with a two-pole K matrix where, however, the parameters f_1, f_2, and s_2 are very large (see Table I). In essence, the K matrix contains a "constant" nonresonating background in addition to the resonance. This is reasonable since the resonance is broad. We remark that the phase in Fig. 8(b) is now remarkably constant above 1.4 GeV, even without a direct production term. The phase difference $\phi(2^+) - \phi(1^+)$ between the A_2 and A_1 waves is in excellent agreement with the data in Fig. 8(d).

In addition to the pleasing behavior of the phase, we notice the following properties of solution E:

(1) The scattering length is much smaller than in solutions A, B, and C. From a theoretical point of view this may be a slight drawback since a_0 now disagrees with current-algebra predictions. However, the solution E has the advantage that

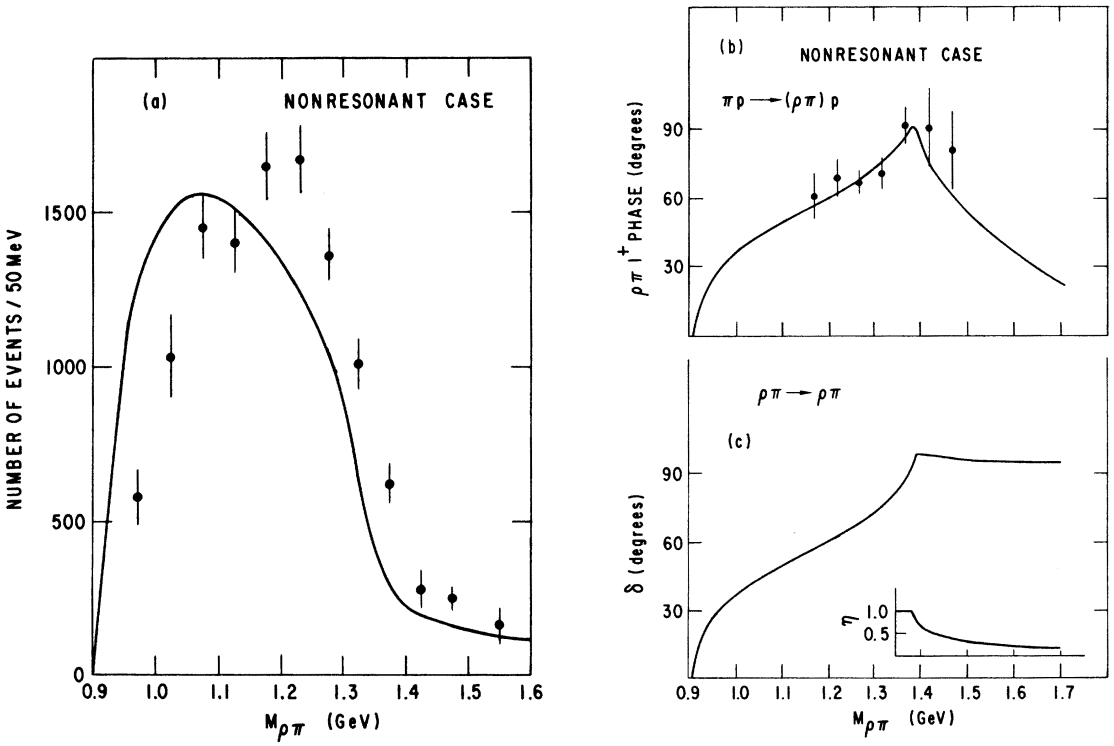

FIG. 9. Our nonresonant solution F described in the text in Tables I and II. Data points in (a) are taken from Ref. 2. The points for the absolute phase of the $J^P = 1^+$ S-wave amplitude in (b) are reconstructed from the experimental difference $\phi(2^+) - \phi(1^+)$, as described in the text. (a) Mass spectrum. The solid line is our solution F, integrated over the range $|t| = 0.1$ to 0.3 GeV^2, as described in the text, and normalized to the data. For absolute normalization, consult Table II. (b) The phase of our 1^+ S-wave $\rho\pi$ amplitude in $\pi p \rightarrow (\rho\pi)p$. (c) The phase-shift and (inset) inelasticity parameters of the $\rho\pi \rightarrow \rho\pi$ S-wave amplitude as computed from our model F.

the mass spectrum is now depleted at low values of M compared to solutions A, B, and C, in better agreement with the data. Solution E fits the combined mass spectrum of the 25- and 40-GeV/c data[2] very well. The reason is that since a_0 is small, the Deck amplitude is not enhanced at low M. While it may be dangerous to assign too much weight in the analysis to the low-M points, the solution is nevertheless attractive.

(2) As a consequence of this low value of a_0, the A_1 mass is now smaller, ~1.2 GeV, while its width is still of the order of 400 MeV.

(3) The phase shift δ of the $\rho\pi \to \rho\pi$ amplitude shown in Fig. 8(c) crosses 90° at a value of M considerably higher than the resonance position, $M \simeq 1.2$ GeV, which we determine from the location of the second-sheet pole. We note, however, that the rate of increase of δ is greatest near $M = 1.2$ GeV.

(4) We notice that inelasticity plus the nonresonant background also lead to a better fit of the mass spectrum in Fig. 8(a) above 1.4 GeV.

(5) Finally, in Fig. 8(f) we show the $K^*\overline{K}$ cross section that we compute. We call attention to the enhancement and peak near threshold. In this respect, it is relevant to remark that a dominant $J^P = 1^+$ S-wave component has been identified near the $K^*\overline{K}$ threshold in data[17] on $\pi^- p \to K^{*0} K^- p$ at 16 GeV/c. Accordingly, our use of this channel as a source of inelasticity for the A_1 has direct experimental support. Refined measurements of the $K^*\overline{K}$ channel would be useful, both for establishing the parameters of the A_1 resonance and for determining the amount of direct production.

6. *Nonresonant alternative*

To end this section, we discuss briefly the possibility of a nonresonant amplitude, i.e., an amplitude with no A_1 resonance. The main argument for this has been, traditionally, the absence of any strong phase variation in the $J^P = 1^+$ S-wave $\rho\pi$ amplitude in the $\pi p \to (\rho\pi)p$ reaction. Before displaying a solution in which the phase is fitted without a resonance, we record a few observations. Independent of the variation of the phase with mass, the data show that the $\rho\pi$ phase reaches ~70 to 90° near 1300 MeV, i.e., the elastic $\rho\pi$ phase must be appreciable even before the inelastic thresholds. The only way to obtain a strong phase with no resonance is to have a large value for the scattering length a_0. However, if a_0 is large, one expects a large enhancement of the Deck amplitude near threshold, and therefore an incorrect shape for the mass spectrum. This is perfectly borne out by solution F, shown in Fig. 9. We have adjusted the phase in order not to have a resonance. The behavior of the phase is very satisfactory, but the mass spectrum is unacceptable, much too enhanced near threshold. Is this a safe argument at present for discarding the possibility of a nonresonating amplitude? Not quite, of course, but we feel confident that the existence of the resonance is more probable than its nonexistence. With data of slightly better quality one may be able to rule out a nonresonating amplitude completely.

V. CONCLUSIONS AND DISCUSSION

In this article, we developed an essentially new method and applied it to the phenomenological analysis of diffractive data on $\pi p \to (\rho\pi)p$ at high energies. We demonstrated that our Deck model modified in a well-defined way by the requirements of unitarity in the $(\rho\pi)$ system leads to an excellent explanation of the data. There are few free parameters in our approach. Moreover, all of these parameters are connected intimately with the behavior of the $\rho\pi \to \rho\pi$ $J^P = 1^+$ S-wave scattering amplitude, whose physical characteristics it has been our ambition to extract from the diffractive data. The parametrizations allow either for the presence of an A_1 resonance in the $J^P = 1^+$ $\rho\pi$ system, or for the absence of this long-sought and most enigmatic of the resonances of the conventional quark model. Concluding from our best solutions, we find it most probable that the A_1 resonance does exist, and that it is broad. With the present data we determine a mass and width of 1.3 ± 0.15 GeV and 0.4 ± 0.1 GeV, respectively. These figures are based on the location of the second-sheet pole of our $\rho\pi$ scattering amplitude, and represent rough averages of the specific values we determined from individual solutions. We cannot exclude the nonresonant alternative completely, but we judge it an unlikely solution. Better data should be decisive, and we provide specific suggestions below.

Some of the most important new ingredients of our unitary and analytic approach are listed here:

(a) Incorporation of inelasticity. We accomplish this with a coupled-channel framework, including both the $\rho\pi$ and $K^*\overline{K}$ decay channels. Inelasticity permits the phase $\phi(1^+)$ of the $J^P = 1^+$ $\rho\pi$ wave in $\pi p \to (\rho\pi)p$ to cease its rapid growth with mass at and above 1.4 GeV, owing to the different form of the Watson final-state-interaction theorem above inelastic thresholds. The inelasticity required by the data is consistent with the SU(3) expectation that the ratio of A_1 coupling strengths $g_{\rho\pi}/g_{K^*\overline{K}} = \sqrt{2}$.

(b) Unitary parametrizations of the $J^P = 1^+$ $\rho\pi \to \rho\pi$ scattering amplitude which include not only a resonance pole but also nonresonant background in the

same partial wave. Our best solution E suggests that the background may be significant.

(c) Incorporation of some direct diffractive production of the A_1 resonance, in addition to the unitarized Deck production. The proportion of direct production and its t_1 dependence could be determined from a careful analysis of more accurate data. At the present time, our solutions show a wide latitude for the fraction of direct production. The unitarized Deck term is always dominant.

(d) Mass-slope correlation. A property of both the data and of our Deck production model, the logarithmic slope of the production momentum transfer distribution $d\sigma/dt_1$ decreases dramatically as M increases. One practical consequence is that the position of the peak in $d\sigma/dM$ changes for different selections on $|t_1|$. A proper analysis of the data, and conclusions regarding the position and width of the A_1 resonance, not to mention its existence, require a proper treatment of the mass-slope correlation.

(e) The 2^+-1^+ phase difference. We take seriously the data on the phase difference between the $J^P = 2^+$ D-wave $\rho\pi$ and $J^P = 1^+$ S-wave $\rho\pi$ systems. This crucial information has generally been ignored in earlier analyses.

It is interesting to compare the state of our understanding of $\rho\pi$ scattering, as we now view it, with that of $\pi\pi$ scattering.[18] In both cases, unitary analytic coupled-channel partial-wave analyses are required.[19] For $\pi\pi$ scattering, the $K\overline{K}$ threshold effect is very important. Similarly, in our A_1 analysis, we showed that the coupling to $K^*\overline{K}$ is significant. However, the production mechanisms are different. Analyses of $\pi\pi$ scattering are based on data in which one of the "incident" pions is an off-the-mass-shell exchanged pion. In our A_1 analysis, the "exchange" is a Pomeron, and (in a loose sense) we study $\pi P \to \pi\rho$ and $\pi P \to K^*\overline{K}$. Neither case is without its technical complications. Because of complicated spin dependence, competition from A_1 exchange, and absorptive effects, the "data" on $\pi\pi$ scattering are obtained through model-dependent extrapolations to the exchanged-pion pole. Indeed, an extrapolation must be performed in order to permit extraction of the $\pi\pi$ phase shifts. To some degree, the Deck production mechanism in the A_1 case is better understood and easier to deal with than are the production related complexities in $\pi\pi$ scattering. The observed helicity properties of the A_1, predominantly t-channel helicity zero, and the strong mass-slope correlation of the production momentum-transfer distribution are correctly predicted by the Deck model.[6]

Our analysis of the data shows that it is the unitarized Deck term which dominates in $\pi p \to (\rho\pi)p$, and not the term representing direct production of the A_1. Because the Deck amplitude is dominant and sufficiently well known, we believe that any phase and elasticity assignments for the strong-interaction $\rho\pi \to \rho\pi$ amplitude can be verified not only by confronting $\phi(1^+)$, the phase of the $J^P = 1^+$ part of $\pi p \to (\rho\pi)p$, but also by checking the shape and magnitude of the differential cross section $d\sigma/dt_1 dM$. To be sure, there are some unresolved problems associated with diffractive production. We may mention the pronounced structure observed near $|t_1| = 0.2$ GeV^2 in some inelastic diffractive processes.[20] It is not known whether such structure is present when the $J^P = 1^+$ S-wave $\rho\pi$ system is extracted from data on $\pi p \to (\rho\pi)p$. However, if so, it would not be explained by our simple unabsorbed Deck model. For this and other reasons, we would prefer to work with data on $\pi p \to (\rho\pi)p$ as close to $t_1 = 0$ as possible, and ideally, with differential cross sections and phases extrapolated to $t_1 = 0$. Nevertheless, in the A_1 case, the dependence of cross sections and phases on t_1 is of potential interest in itself. For example, with enough good data, analyzed with our method as a function of mass in different narrow intervals of t_1, we could identify differences between the t_1 dependences of the Deck and direct production terms. In some models,[1] the direct production term is expected to vanish as $t_1 \to 0$. Such subtleties are lost in the present data, which neither reach small enough t_1 nor are of sufficient statistical quality to permit an analysis more differential than we have performed.

The data analyzed in this article are based on a sample of 43×10^3 events of $\pi p \to (\rho\pi)p$ obtained at 40 GeV/c by the CERN-IHEP[2] collaboration. While representing the highest statistics available at a single energy, these data are nevertheless so scant that the intervals in mass and momentum transfer in which results are presented are 50 MeV and 0.3 GeV^2, respectively. An analysis based on roughly 10^6 events would permit more refined conclusions, perhaps providing more convincing evidence for phase variations as a function of both mass and momentum transfer. As remarked above, it would be useful if the point $t_1 = 0$ were accessible, with absolute normalization. The low-mass part of the spectrum $d\sigma/dt_1 dM$ was shown to play an important role in the selection of our solutions, in the determination of the scattering length a_0, and, as a consequence, in the specification of the A_1 mass and width (as well as its very existence). Thus, good data at small M are needed, in several reasonably small intervals of t_1. This latter point is important because of the strong mass-slope correlation.

We demonstrated that the $K^*\overline{K}$ channel is an im-

portant second decay channel for the A_1. Thus, we also advocate a detailed study of $\pi p \to (K^*\overline{K})p$ at high energy. It would be useful to be able to incorporate into our analysis measurements of the mass and momentum-transfer dependences of the phase $\phi(1^+)$ and differential cross section for the $J^P = 1^+$ S-wave $K^*\overline{K}$ system from $\pi p \to (K^*\overline{K})p$. We discovered that with present data the two regions $M < 1.4$ GeV and $M \gtrsim 1.4$ GeV can be treated independently to some degree, in the sense that many amplitudes can be constructed with approximately the same characteristics for $M < 1.4$ GeV, but very different behavior above. Once better data are available above $M = 1.4$ GeV on the $J^P = 1^+$ $\rho\pi$ and $K^*\overline{K}$ systems from both $\pi p \to (\rho\pi)p$ and $\pi p \to (K^*\overline{K})p$, a well defined preferred solution may be selected up to perhaps $M = 1.8$ GeV.

We have concentrated on diffractive production of the A_1. Nondiffractive reactions such as $\pi^- p \to (\rho\pi)^0 n$, $K^- p \to (\rho\pi)^0 \Lambda$, and $\overline{K}p \to (K^*\overline{K})\Lambda$ require a somewhat different analysis. In these processes, the exchange is presumably either a "ρ" or a "K^*" The data permit a study of $\pi'' \rho'' \to \pi\rho$, $\overline{K}'' K^{*\prime\prime} \to \rho\pi$, and $\overline{K}'' K^{*\prime\prime} \to K^*\overline{K}$, in the absence of diffractive production. In our treatment of unitarity for the diffractive processes $\pi p \to (\rho\pi)p$ and $\pi p \to (K^*\overline{K})p$ in Sec. III, we consider only two-body intermediate states in the unitarity equation. Thus, the multiparticle contribution $\pi P \to \pi P$ is excluded. Our unitarity constraint on $\pi P \to \pi\rho$ and $\pi P \to K^*\overline{K}$ has a linear form. For the nondiffractive processes, this simplification is not permissible. As a result, except for coupled-channel effects, and for complications owing to its large width, nondiffractive production of the A_1 should show the resonant $e^{i\delta}\sin\delta$ behavior as a function of mass which Fox conjectured.[1] The curves which represent our direct production contributions in Figs. 4–8 are thus illustrative of our expectations for the shape of the $I = 1$ $J^P = 1^+$ component of $d\sigma/dM$ in nondiffractive processes. They all show a broad featureless spectra, consistent with our conclusion that the A_1 is a wide resonance. The *phase* of the $J^P = 1^+$ S-wave $I = 1$ amplitude observed in the charge-exchange reaction $\pi^- p \to (3\pi)^0 p$ should be that shown in Figs. 5(c), 6(c), or 8(c), if ρ exchange dominates. Obviously, a careful spin-parity analysis of high-statistics nondiffractive data at high energy would be instructive. Low-energy results may suffer from serious ambiguities owing to the influence of overlapping competing channels. The present data[16] are consistent with our expectations. We may remark in passing that the long-ignored processes $\overline{K}p \to (K^*\overline{K})\Lambda$ and $Kp \to (K^*\overline{K})\Sigma$ could be a rich source of information not only on the A_1 but also on the lost mesons with $I = 0$ in the $J^{PC} = 1^{++}$ and 1^{+-} nonets.

Our A_1 resonance is broad. As a result, controversy may arise concerning the determination of its parameters from physical region data, according to the different forms proposed for its parametrization. Because of its breadth, the A_1 may also be subject to the same ambiguities of interpretation which plague the broad candidates for membership in the 0^{++} multiplet, such as the ϵ and κ. It is interesting that the mass of our A_1 places it close to the A_2. In no sense have we "hidden it under" the A_2. As we explained in Sec. III, the mass of our A_1 is determined by the sharp drop observed in the $J^P = 1^+$ component of $d\sigma/dM$ between $M = 1.2$ and 1.4 GeV. The proximity in masses of the A_2 and A_1 is not unexpected since both are $l = 1$ excitations in the quark model.

In the near future we expect to return to our study of the Q mesons,[4] using a method of analysis similar to that developed here. When justified by the desire for precise quantitative agreement with new future data on the A_1, some improvements and refinements of our present approach may be investigated. The Deck amplitudes can be refined in various ways. For example, the true S-wave projection could be calculated for $|t_1| > 0$, instead of our approximate form, Eq. (2.3). Similarly, the vector-pseudoscalar scattering amplitudes ($\rho\pi \to \rho\pi$, $K^*\overline{K} \to K^*\overline{K}$, and $\rho\pi \to K^*\overline{K}$) can be parameterized in a more sophisticated fashion. We could also incorporate more channels, such as the $\epsilon\pi$ P wave, the $K^*\overline{K}$ and $\rho\pi$ D waves, the $\rho\omega$ S and D waves, the $f\pi$ P wave, and so forth. It would be interesting to examine the small $J^P = 1^+$ $\rho\pi$ and $K^*\overline{K}$ amplitudes with t-channel helicity $|\lambda_t| = 1$. One may also wish to include a more complete description of the forces in the $\rho\pi$ system, through an N/D formalism, for instance, as mentioned in Sec. II. As an example, we may consider the pion-exchange diagrams shown in Fig. 10. A calculation along these lines was reported by Longacre and Aaron.[21] They include three-body effects by the use of separable two-body amplitudes. While the actual $\pi\pi(K^*\overline{K})$ amplitudes (particularly the $I = 0$ S wave $\pi\pi$) may be much more complicated than their choices,[18] at least the finite widths of the ρ, ϵ, and K^* resonances are taken into account in a reasonable manner. They conclude that the pion-exchange diagrams provide only a small contribution. In comparison, our point of

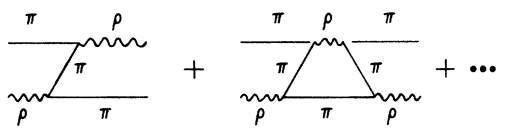

FIG. 10. Pion-exchange diagrams in $\rho\pi$ scattering.

view has been to parameterize the $\rho\pi \to \rho\pi$ scattering amplitude phenomenologically and then to determine the parameters from the data. The dynamical explanation of the values which these parameters take on is another question with which we are not primarily concerned. This procedure is analogous to that followed in $\pi\pi$ scattering. We remark that the results of Ref. 21 cover a smaller range in M than ours, and that our amplitudes fit the data much better with fewer parameters. Perhaps the conclusion that the A_1 has a mass as great as 1.5 GeV is connected with the neglect in Ref. 21 of the $K^*\overline{K}$ and other inelastic channels which open above $M = 1.4$ GeV. Nevertheless, it is certain that in future analyses, we will have to depart from the two-body approximation which we have made, and incorporate smearing of the results associated with the ρ and K^* widths.

While sharing some features in common with an earlier analysis of the A_1 by Bowler *et al.*,[22] our work differs significantly in at least three respects. Our Deck amplitudes are well defined and constrained. Our approach is formally and physically different in that we employ a two-channel method. We do not postulate an *ad hoc* phase difference of 40° between the Deck and direct terms, and our direct term plays little role.

Given the existence of an A_1, it presumably lies on a Regge trajectory which, if roughly parallel to the ρ and A_2 trajectories, will intersect $t = 0$ near $\alpha_{A_1}(0) = -0.5$. Evidence for such an unnatural-parity trajectory has recently been found in polarization measurements in $\pi^- p \to \pi^0 n$ at 17 GeV/c (Ref. 23) and in data on $\Delta\sigma_L$ in pp scattering at 6 GeV/c at Argonne.[24]

ACKNOWLEDGMENT

We are grateful to Dr. G. Mennessier, CERN, for valuable discussions and for his early collaboration.

APPENDIX

In this Appendix, we present a heuristic argument to support our claim that Eq. (3.5) is the proper definition of a production amplitude corrected by unitarity, or final-state interactions.

In potential scattering, for instance, two types of resonance may be distinguished. A resonance may arise when the forces between scattering particles are sufficiently strong. We use the term *dynamical* resonance to identify this situation There is a second type of resonant scattering which is encountered frequently. It occurs when a bound state of a Hamiltonian H_0, with energy E_0, is weakly coupled to a continuum by some Hamiltonian H_1, thereby becoming unstable.[25] The continuum is the two-particle decay sector of interest to us here. In this latter case, we call the resonance an ***unstable*** state. It is also called a CDD pole by dispersion theorists. According to our terminology, the resonance of the quark model are examples of these *unstable* states.

For resonances in the *dynamical* class, there is no ambiguity in the specification of the final-state interactions.[25] The phase shifts obey Levinson's theorem, and Eq. (3.5) provides the correct answer. For ***unstable*** states, however, it is recognized that the solution to the unitarity equation is ambiguous. An extra prescription is required.

We consider the problem of an unstable state, labeled "ρ" for definiteness, which is coupled to two continua. We label these continua "$\pi\pi$" and "e^+e^-". We suppose that the coupling to $\pi\pi$ is much greater than to e^+e^-. Thus, the ρ width is due mainly to the $\rho\pi\pi$ coupling. We are interested in obtaining an expression for the amplitude for $e^+e^- \to \pi\pi$, which is assumed to be a relatively weak process. It can be shown in formal scattering theory that Eq. (3.5) emerges as the appropriate answer.[9] We shall not expound the argument here, but we present instead an intuitive justification for the result.

We assume for simplicity that the unstable ρ is an S-wave $\pi\pi$ and e^+e^- state. Let f be the $\rho\pi\pi$ coupling strength and let α be the ρe^+e^- coupling strength. We denote by β the value of the ***bare***, pointlike coupling $e^+e^- \to \pi\pi$. These three primitive interactions are represented in Fig. 11. For simplicity, we suppose that no other couplings are present. As remarked above, we assume that $f \gg \alpha$ and $f \gg \beta$.

According to our hypotheses, $\pi\pi$ scattering occurs only through the ρ. Thus, the $\pi\pi$ amplitude may be written, to lowest order in α and β, as

$$t_{\pi\pi}(s) = \frac{f^2}{m_\rho^2 - s - f^2 C(s)} = \left(\frac{s}{s - 4m_a^2}\right)^{1/2} e^{i\delta} \sin\delta. \tag{A1}$$

This expression is obtained easily upon summing the series illustrated in Fig. 12. Here $C(s)$ is the Chew-Mandelstam function for $\pi\pi$. Equation (A1)

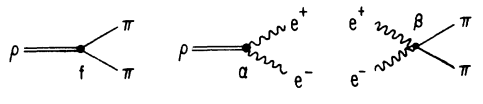

(a) (b) (c)

FIG. 11. Primitive interactions in our simple model: (a) $\rho\pi\pi$ coupling vertex. (b) ρe^+e^- coupling vertex. (c) $e^+e^- \to \pi\pi$ coupling vertex.

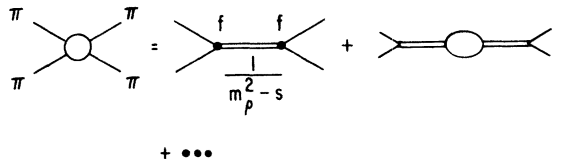

FIG. 12. $\pi\pi \to \pi\pi$ amplitude in our simple model.

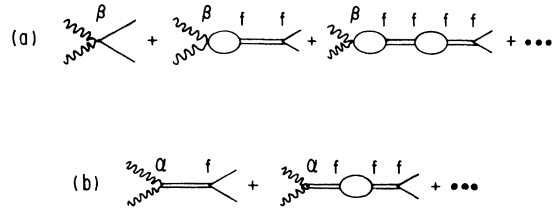

FIG. 13. $e^+e^- \to \pi\pi$ amplitude in our simple model: (a) The component in which the $\pi\pi$ system interacts in the final state. (b) The direct resonance production component.

shows that the ρ has been moved into the complex plane and has acquired a width as a result of the rescattering series.

There are two contributions to the amplitude for $e^+e^- \to \pi\pi$, shown in Figs. 13(a) and 13(b). The first contribution, Fig. 13(a), is the sum of the primitive bare coupling and of its attendant $\pi\pi$ final-state rescattering series. To first order in α and β, this sum is

$$t^{\text{fsi}}(e^+e^- \to \pi\pi) = \frac{\beta(m_\rho^2 - s)}{m_\rho^2 - s - f^2 C(s)} . \qquad \text{(A2)}$$

The second contribution is a term in which the ρ is *directly* produced and decays subsequently into $\pi\pi$, Fig. 13(b). This direct series leads to the amplitude

$$t^{\text{direct}}(e^+e^- \to \pi\pi) = \frac{\alpha f}{m_\rho^2 - s - f^2 C(s)} . \qquad \text{(A3)}$$

The relative size of the two contributions (A2) and (A3) is determined by the ratio of the parameters α and β. Depending on the particular physical situation, one or the other may dominate, or they may be comparable. It is clear that (A2) and (A3) have very different properties. Owing to the zero at $s = m_\rho^2$, the final-state-interaction amplitude (A2) behaves approximately as $e^{i\delta}\cos\delta$ in the vicinity of the resonance position. By contrast, the direct amplitude (A3) behaves roughly as $e^{i\delta}\sin\delta$. If Eq. (A2) is dominant, then the existence of the resonance is signaled by a *dip* in the mass spectrum near $s = m_\rho^2$ not by the traditional peak.[26]

Our separation of the $e^+e^- \to \pi\pi$ amplitude into two components is transparent in the simple model described here. We may now compare Eqs. (3.9), (3.11), and (3.12) of Sec. III, with (A1), (A2), and (A3), respectively. Their complete similarity is our heuristic justification for asserting that our Eq. (3.5) is the proper definition of a production amplitude corrected by final-state interactions, whether the resonance is a dynamical effect or an unstable state.

Similar arguments have been advanced by Pumplin[27] and by Bauer.[28]

---

†Permanent address; work performed under the auspices of the U. S. Energy Research and Development Administration.

*Postal Address: LPTHE Tour 16-1er étage, 4 Place Jussieu, 75230 Paris, France.

[1]For reviews consult J. Rosner, in Plenary Session Report, *Proceedings of the XVII International Conference on High Energy Physics, London, 1974*, edited by J. R. Smith (Rutherford Laboratory, Chilton, Didcot, Berkshire, England, 1974); and G. C. Fox, in *Experimental Meson Spectroscopy—1972*, proceedings of the Third International Conference, Philadelphia, edited by A. H. Rosenfeld and K.-W. Lai (AIP, New York, 1972).

[2]Yu. M. Antipov *et al.*, Nucl. Phys. B63, 153 (1973); G. Ascoli *et al.*, Phys. Rev. D 7, 669 (1973).

[3]E. Berger, in *Proceedings of the Daresbury Conference on Three-Particle Phase Shift Analysis and Meson Resonance Production, 1975*, edited by J. Dainton and A. J. G. Hey (Science Research Council, Daresbury, 1975).

[4]J. L. Basdevant and E. L. Berger, Phys. Rev. Lett. 37, 977 (1976), and references listed therein.

[5]O. Babelon, J. L. Basdevant, D. Caillerie, and G. Mennessier, Nucl. Phys. B113, 445 (1976), and references cited therein.

[6]E. L. Berger and J. T. Donohue, Phys. Rev. D 15, 790 (1977).

[7]K. N. Watson, Phys. Rev. 88, 1163 (1952).

[8]R. L. Warnock, Nuovo Cimento 50, 894 (1967); Nuovo Cimento 52A, 637 (1967).

[9]J. L. Basdevant (unpublished).

[10]J. Ballam *et al.*, Phys. Rev. D 5, 545 (1972); Y. Eisenberg *et al.*, *ibid.* 5, 15 (1972).

[11]More quantitatively, it is observed that $\sigma(J^P) \propto p_{\text{lab}}^{-n}$, with $n = 0.40 \pm 0.06$ for $J^P = 1^+$ and $n = 0.51 \pm 0.05$ for $J^P = 2^+$. Theoretically, the Regge phase-energy relationship specifies that the production amplitude $A(J^P) \propto s^\alpha \exp(-i\pi\alpha/2)$. Thus, the difference $\Delta n = 2\Delta\alpha$, and Δn may be converted to a difference of the production phases, $\Delta\phi_{\text{prod}} = \pi n/4$. We deduce $\Delta\phi_{\text{prod}} \simeq 5 \pm 5°$.

[12]J. D. Jackson, Nuovo Cimento 34, 1644 (1964). For parameters, consult CCNY-BNL Collaboration, M. Margulies *et al.*, Phys. Rev. D 14, 667 (1976).

[13]Without the cutoff factor, $\phi(A_2) \to 90°$ for $M \gg M_{A_2}$, which is undesirable. Indeed, without the cutoff, $\phi(A_2)$ reaches only 134° before beginning to descend at $M = 1.5$ GeV. Unfortunately, no A_2 cutoff is used in the fits done in Ref. 2, which contributes to the impression that $\phi(1^+)$ shows no phase variation in the

region $1.2 < M < 1.5$ GeV.
[14]R. L. Schult and H. W. Wyld Jr., Phys. Rev. D 16, 62 (1977).
[15]S. Weinberg, Phys. Rev. Lett. 17, 616 (1966).
[16]M. J. Emms *et al.*, Phys. Lett. 60B, 109 (1975); F. Wagner, M. Tabak, and D. M. Chew, *ibid.* 58B, 201 (1975); Amsterdam-CERN-Nijmegen-Oxford Collaboration [$K^-p \to (3\pi)\Lambda$ at 4.2 GeV/c], CERN report submitted to the Tbilisi Conference, 1976 (unpublished).
[17]Aachen-Berlin-Bonn-CERN-Heidelberg Collaboration, G. Otter *et al.*, Nucl. Phys. B96, 365 (1975). See also R. Diamond *et al.*, Phys. Rev. D 7, 1977 (1973).
[18]J.-L. Basdevant, C. D. Froggatt, and J. L. Peterson, Nucl. Phys. B72, 413 (1974).
[19]Recently, the importance of a coupled-channel treatment of the $\pi\eta$ and $K\bar{K}$ systems has been stressed by S. M. Flatté, Phys. Lett. 63B, 224 (1976).
[20]For a summary of the data and for a phenomenological analysis, consult R. Cutler and E. L. Berger, Phys. Rev. D 15, 1903 (1977).
[21]R. S. Longacre and R. Aaron, Phys. Rev. Lett. 38, 1509 (1977).
[22]M. G. Bowler *et al.*, Nucl. Phys. B97, 227 (1975).
[23]CERN-Munich Collaboration, H. Becker *et al.*, paper submitted to the Tbilisi Conference, 1976 (unpublished).
[24]I. P. Auer *et al.*, Phys. Lett. 67B, 113 (1977); and private communications.
[25]See, for instance, M. L. Goldberger and K. M. Watson, *Collision Theory* (Wiley, New York, 1964).
[26]L. Resnick, Phys. Rev. D 2, 1975 (1970).
[27]J. Pumplin, Phys. Rev. D 2, 1859 (1970).
[28]T. Bauer, Phys. Rev. Lett. 25, 485 (1970).